Louisiana State University

LSU Scholarly Repository

1999

Precursors for Chemical and Photochemical Vapor Deposition of Copper Metal.

Alicia Marie James
Louisiana State University and Agricultural & Mechanical College

Follow this and additional works at: https://repository.lsu.edu/gradschool_disstheses

Recommended Citation

INFORMATION TO USERS

This manuscript has been reproduced from the microfilm master. UMI films the text directly from the original or copy submitted. Thus, some thesis and dissertation copies are in typewriter face, while others may be from any type of computer printer.

The quality of this reproduction is dependent upon the quality of the copy submitted. Broken or indistinct print, colored or poor quality illustrations and photographs, print bleedthrough, substandard margins, and improper alignment can adversely affect reproduction.

In the unlikely event that the author did not send UMI a complete manuscript and there are missing pages, these will be noted. Also, if unauthorized copyright material had to be removed, a note will indicate the deletion.

Oversize materials (e.g., maps, drawings, charts) are reproduced by sectioning the original, beginning at the upper left-hand corner and continuing from left to right in equal sections with small overlaps. Each original is also photographed in one exposure and is included in reduced form at the back of the book.

Photographs included in the original manuscript have been reproduced xerographically in this copy. Higher quality 6" x 9" black and white photographic prints are available for any photographs or illustrations appearing in this copy for an additional charge. Contact UMI directly to order.

UMI®

Bell & Howell Information and Learning
300 North Zeeb Road, Ann Arbor, MI 48106-1346 USA
800-521-0600

PRECURSORS FOR CHEMICAL AND PHOTOCHEMICAL VAPOR DEPOSITION OF COPPER METAL

A Dissertation

Submitted to the Graduate Faculty of the
Louisiana State University and
Agricultural and Mechanical College
in partial fulfillment of the
requirements for the degree of
Doctor of Philosophy

in

The Department of Chemistry

by
Alicia M. James
B.S. Southern University and A&M College, 1992
May, 1999

UMI Number: 9936095

UMI Microform 9936095
Copyright 1999, by UMI Company. All rights reserved.

This microform edition is protected against unauthorized
copying under Title 17, United States Code.

UMI
300 North Zeeb Road
Ann Arbor, MI 48103

To God and my family

ii

Acknowledgements

All praises to my Lord and Savior, Jesus Christ for giving me the strength to face and overcome the obstacles that were before me during the duration of graduate school. Lord, thank you for the trials and tribulations because you state in your word, "I can do all things through Christ that strengthens me."

I thank God for my family. Words can not express the love and gratitude I have for them. They have shown me that anything worth having is worth fight for.

I would like to thank Dr. Maverick for his infinite amount of patience, understanding, and knowledge. Under his tutelage, I have learned to be an effective writer, communicator, as well as a chemist.

A great appreciation to my advisory committee members, Dr. Leslie Butler, Dr. Gregory Griffin, Dr. Robin McCarley, and Dr. Chan for their valuable insight and critiques of my work. An enormous amount of gratitude to Dr. Tracey McCarley and Laura Baker for the exact mass measurements in a short period of time and to Dr. Frank Fronczek for all the crystal structures.

I would like to thank Muna Bufaroosha, Sylvester Burton, and Zuzanna Cygan for their words of encouragement; a special thanks to Hui Fan for his help in making the analyses of the copper metal films. I also want to thank all of those individuals, so numerous to name, for their many acts of kindness and support during my time in graduate school.

Last but not least, I thank God for Anna Shanklin. People come in and out of your life a dime a dozen but true friends last forever. I want to thank her personally for being my strength when I was weak.

iii

Table of Contents

Chapter 3

Properties of Other Tetrameric Copper (I) Amide Clusters

List of Tables

List of Figures

Abstract

The colorless square-planar cluster $[CuN(SiMe_3)_2]_4$, which contains four Cu(I) ions with four bridging amide groups, was studied as a precursor for chemical and photochemical vapor deposition of Cu metal. The cluster phosphoresces in CH_2Cl_2 solution and in the solid state at room temperature. Its electronic spectrum in CH_2Cl_2 consists of two intense bands which are assigned to symmetry-allowed $3d \rightarrow 4p$ transitions; the phosphorescence is also likely to be metal-centered. Solid $[CuN(SiMe_3)_2]_4$ luminesces with approximately the same spectrum as that of the CH_2Cl_2 solutions. At 77 K, the solid-state luminescence red-shifts slightly. The emission lifetime in glassy Et_2O solution is 690 μs. $[CuN(SiMe_3)_2]_4$ deposits Cu metal via chemical vapor deposition under H_2 carrier gas at substrate temperatures of 145-200 °C. Deposition also occurs photochemically beginning at 136-138 °C under near-UV irradiation.

The preparation of monomeric derivatives of $[CuN(SiMe_3)_2]_4$ was attempted by using neutral donor ligands L (e.g. $L_nCu(N(SiMe_3)_2$; L= CO, PR_3, CN-t-Bu; n=1-3). The target compounds were expected to be more volatile than the copper cluster and still maintain photosensitivity. CuCl and $[Cu(CH_3CN)_4]PF_6$ were used as starting materials. Even in the presence of L, $[CuN(Si(Me_3)_2]_4$ is a major product in reactions using CuCl and $NaN(SiCH_3)_2$. $[Cu(CH_3CN)_4]PF_6$ was a promising route for the monomeric Cu(I) complexes because of ready dissociation of its acetonitrile ligands. However, the characterization of these complexes was unsuccessful.

Other Cu(I) amide clusters have been prepared; they may also be suitable for chemical and photochemical vapor deposition of Cu. $[CuNEt_2]_4$, $[CuN(i\text{-}Pr)_2]_4$, and

$[CuN(t-Bu)(SiMe_3)]_4$ are phosphorescent though they are very air sensitive. They should be more volatile and produce Cu metal films more readily than $[CuN(SiMe_3)_2]_4$.

$Cu(hfac)_2$ is a versatile Lewis acid, forming adducts with a variety of bases. The bases that were used were ethylene glycol, 2-methoxyethanol, propylene glycol, and 1-methoxy-2-propanol. Each $Cu(hfac)_2$ adduct deposited Cu metal under H_2 gas at a substrate temperature of 200 °C and a precursor temperature of 80 °C. In contrast to previously known adducts with sample alcohols, the new precursors do not require excess alcohol vapor for stability. Nevertheless, no Cu deposition was observed with these precursors in the absence of H_2 at temperatures up to 135 °C.

x

Chapter 1

Introduction

1.1 Metal Interconnects and Technology

Metals are used in the microelectronics industry as a means of supplying power and transmitting information. They are required to connect the miniature components like transistors, capacitors, resistors and diodes patterned on the silicon wafer that go into making an Integrated Circuit (IC).[1.1] The application of metals and metal-like layers is called metallization. Some of the commonly used metals in Metal Oxide Semiconductor technology for microelectronics are aluminum (Al), tungsten (W), titanum (Ti), and tantalum (Ta). Metal-like layers include polysilicon, silicides of Ti, Ta, and platinum (Pt), and titanium nitride.

Interconnect metallization is used for connecting the devices on the IC itself, and global connections leading out of the IC. The metal of choice is Al, often in alloys with small amounts of Cu and other metals, usually in conjunction with a diffusion barrier. Since interconnect lines are very thin and run over extensive lengths, low resisitivity and high tolerance to electromigration are important requirements.

Enhancement in the performance and speed of ICs can be achieved by reducing the device feature size and thereby the overall size of the IC. Devices such as dynamic random access memory (DRAM), static random access memory (SRAM), and logic devices with high circuit speed, high packing density and low power dissipation require downward scaling of feature size in ultra-large scale integration (ULSI) structures.[1.2] Current feature size for DRAM is in the range of 0.25-0.35 μm. It is expected that by

1

the year 2000, the transistor channel length in state-of-the-art ICs will be 0.18 μm, while microprocessors will pack more than 15 million transistors into an area of ~ 700 mm^2.[1,3]

Improvements in metallization technology are needed to make faster and more reliable IC's by decreasing metallization feature size and using better materials. Using faster transistors can improve IC performance somewhat. However, the overall speed of large, high density chips is not limited as much by transistor speed as by the metal lines or the interconnects that connect them.[1,4] More specifically it is the resistance of the conductors (metal lines) and the capacitance of the insulators (dielectric films) that limit chip speed. The future of IC manufacturing relies heavily on interconnect materials with lower resistivity and lower capacitance dielectric materials.

1.2 Aluminum

Al or an Al alloy is now generally used as the interconnect material in ULSI circuits. Al has relatively low resistivity, good adhesion to dielectrics, overall compatibility with semiconductor processing steps, and long experience in the industry. Some of the properties of aluminum are listed in Table 1.1.[1,5] Aluminum forms a thin protective oxide film that withstands various thermal processes. Its halides are volatile, which makes it suitable for reactive ion etching (RIE). The reliability of aluminum interconnects, however, is a major concern for maintaining the total reliability of advanced ULSI.

Al-based interconnects are susceptible to failures. As interconnect width (feature size) decreases, current density increases, and metal atoms themselves can move along the direction of electron flow, a phenomenon known as electromigration. This can

Table 1.1 Properties of Metals for Use as Interconnects[1,5]

Property	Copper	Aluminum	Tungsten	Silver	Gold
Melting point (°C)	1085	660	3387	962	1064
Resistivity ($\mu\Omega$-cm)	1.67	2.66	5.65	1.59	2.35
Corrosion in air	high	low	low	high	very low
Adhesion to SiO_2	poor	good	poor	poor	poor
Electromigration Resistance	high	low	very high	very low	very high

3

result in the breakdown of electrical connections, or bridging of conductor lines where isolation is required.

High current density can also lead to stress-induced voidage in metal lines. The metal removed tends to build up elsewhere and this lateral extrusion can result in adjacent lines touching each other, leading to a short circuit. Al, with its relatively low melting point (660 °C), is more susceptible to these two types of failures than metals with higher melting points. However, despite these drawbacks, the many attractive features of aluminum have kept it the metal of choice for most interconnect applications.

1.3 Copper

The lower resistivity of copper (1.67 $\mu\Omega$ cm at 22 °C) vs. aluminum (2.66 $\mu\Omega$ cm at 22 °C) makes it a contender for replacing aluminum and aluminum alloys for chip interconnections. It is widely predicted that copper will become the interconnect of choice for ICs fabricated below the 0.25 μm scale.[1.6] Table 1.1 lists some of the important properties of Cu. In addition to lower resistivity, copper has a higher resistance to electromigration than Al. Use of Cu interconnects would increase the maximum operating frequency of devices and allow the use of higher current densities. Also, copper can be deposited by CVD (chemical vapor deposition), with excellent step coverage and good filling of high-aspect-ratio contacts and vias. CVD of copper metal can also be made selective: for example, Awaya et al. demonstrated deposition on metal and metal silicides, and not on SiO_2 and Si_3N_4.[1.7]

One of the major drawbacks of Cu is its fast diffusion in silicon (Si) and drift in SiO_2-based dielectrics, which can cause the deterioration of devices during operation. Hence, a diffusion barrier is necessary between Cu and Si or SiO_2. One of the most

commonly studied diffusion barriers for Cu is TiN. It is chemically and thermodynamically stable and has a high activation energy for the diffusion of metals. This means that a thin barrier layer may be effective in preventing diffusion of Cu.

Another drawback with implementing copper wiring in silicon ULSI devices is that etching of Cu is difficult. This is because copper halides are not as volatile as those of Al. Etching of metal using a chlorine plasma at room temperature is a standard process in the semiconductor industry. Isotropic etching of copper as copper chloride in a plasma reaction yields etching rates of the order of 0.01 μm min^{-1} which are unacceptably slow. This is because the product $CuCl_2$ is not volatile at typical plasma etching temperatures. Farkas et al. devised a modification to the above process by generating CuCl and then reacting the CuCl with an electron-donating ligand, typically an alkyl phosphine. The isotropic etching was done at 25 to 150 °C. The etching rate reported was 1 μm min^{-1}.[1.8] Norman et al. reported Cu CVD using a Cu(I) precursor, Cu(hfac)(VTMS) (where VTMS = vinyltrimethylsilane).[1.9] The also reported a complementary etching process wherein they could etch deposited Cu by the addition of H(hfac) ligand. Etching rates of 5 μm min^{-1} were reported.

In the isotropic etching process described above, Cu metal is removed from a nonspecific area, in all directions. Therefore, selectivity is compromised. Also, etching can cause microscopic damage to the metal surface.[1.10] Kaanta et al. developed an alternative to RIE which is known as the damascene process for copper interconnect formation.[1.11] In the damascene process an insulator is dry-etched to form trenches conforming to the wiring pattern (Figure 1.1). Once the adhesion/barrier layer (TiN) is deposited, the trenches are then plugged with copper deposited by CVD. Then

Via Oxide Pattern (Black)

TiN(dark gray)/ Cu(gray)CVD

CMP
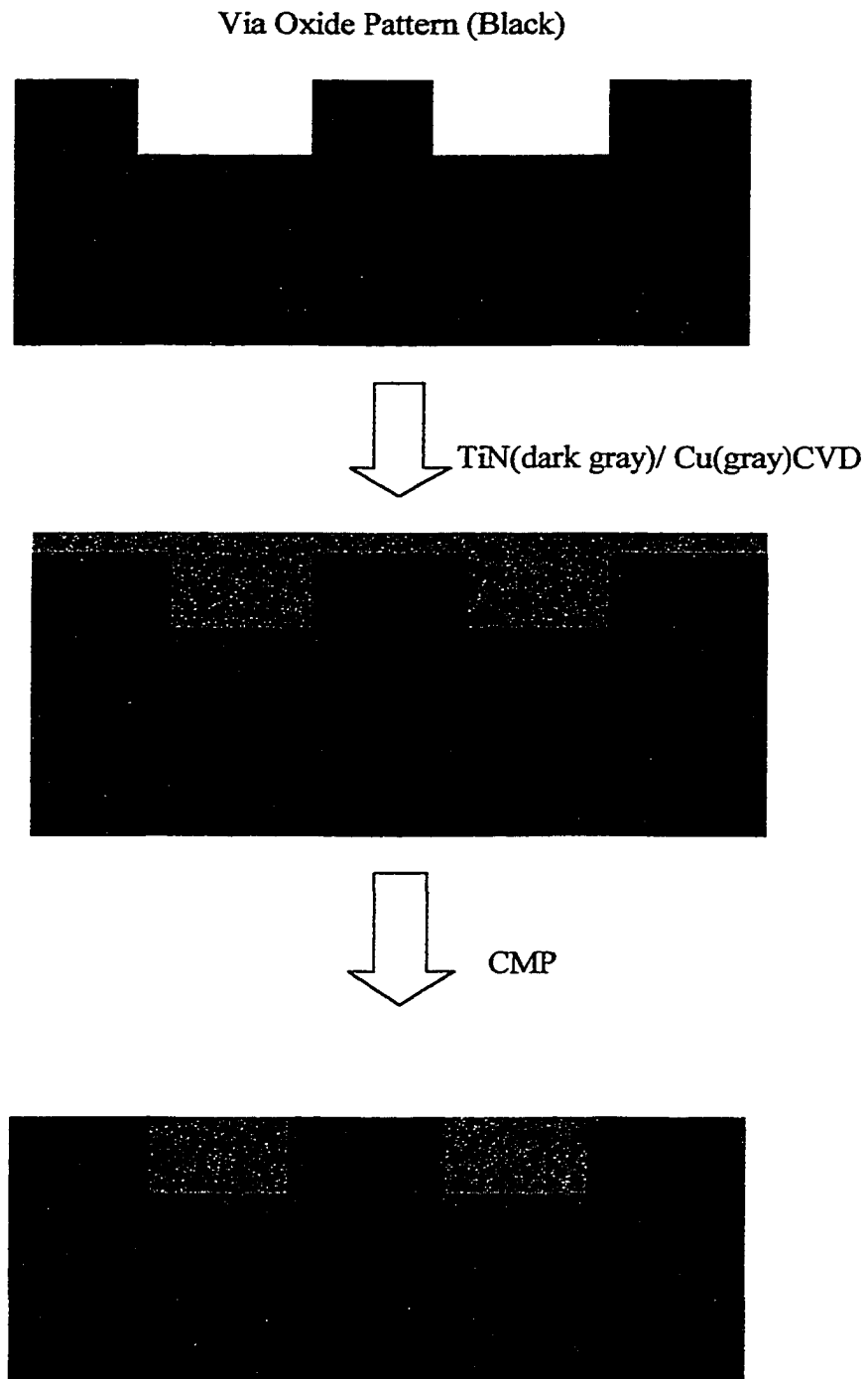
Figure 1.1 Schematic Diagram of a Damascene Process

7

the application of chemical-mechanical polishing (CMP) of the copper down to the insulator yields copper interconnects surrounded by the insulator. The damascene process avoids copper oxidation and diffusion more effectively than RIE because the side walls and bottom surfaces of copper interconnects are already covered by an adhesion/barrier layer such as TiN.

1.4 Chemical Vapor Deposition

Cu-based interconnects will represent the future trend in the deep submicron regime. Cu can be deposited by plating (such as electroless and electrolytic), sputtering (physical vapor deposition, PVD), laser-induced reflow, and CVD. Table 1.2 lists the properties of Cu films obtained by different deposition methods.[12]

Plating-based deposition (electroless and electrolytic) can provide high deposition rates and low tool cost, but the by-products from the reaction can cause environmental problems. This may limit the use of electrochemically deposited copper metal. Cu PVD is a conventional technology with high deposition rate, but poor via-filling and step coverage are the concerns. The laser reflow technique exhibits less compatibility with current ULSI processing. Based on these comparisons, Cu CVD is an attractive approach for copper-based interconnects in ICs. Cu CVD is very good in step coverage and filling high aspect ratio holes. It also gives films that have a resistivity close to that of bulk Cu. This process involves the formation of the Cu film on a heated surface by means of a chemical reaction. The overall process is 1) adsorption of a reactant onto the heated surface, 2) thermal decomposition of the reactant to metal, and 3) desorption of the reaction by-products.

Reproduced with permission of the copyright owner. Further reproduction prohibited without permission.

Table 1.2 Properties of Copper Obtained by Different Deposition Methods[1,12]

	CVD	PVD	Laser Reflow	Electroless	Electrolytic
Resistivity ($\mu\Omega$ cm)	≥ 2	1.75-2	2.6	~2	~2
Impurities	C, O	Ar	-	seed layer	-
Deposition Rate (nm/min)	~100	≥ 100	-	≤ 100	~200
Process Temp (°C)	~250	RT	melt	50-60	RT
Step Coverage	good	fair	-	good	good
Via-Filling Capacity	good	poor	good	fair-poor	fair-poor
Environmental Impact	good	good	good	poor	poor

1.5 Cu CVD Precursors

Copper CVD precursors must possess thermal stability and adequate volatility, yet decompose to high purity metal at temperatures below 300 °C. The physicochemical properties of the precursors play a critical role in the CVD process because they determine the vapor pressure, the adsorption/desorption behavior, the decomposition temperature, the chemical reaction pathways, the purity of the deposited metal, and in many cases, the rate of thin film formation. These combined chemical and physical properties are a direct result of the precursor molecular structure.

Two of the most useful families of copper CVD precursors that have been studied recently are the Cu(I) and Cu(II) β-diketonates (Figure 1.2). The β-diketonate ligand most commonly used in these precursors is hexafluoroacetylacetonate or hfac⁻. Cu(II) precursors generally require the use of an external reducing agent such as hydrogen to deposit copper metal films that are largely free of impurities (Equation 1.1).

$$Cu^{(II)}(hfac)_2 + H_2 \rightarrow Cu(s) + 2hfacH(g) \qquad \text{(Equation 1.1)}$$

The Cu(I) precursors can deposit pure copper films without the use of an external reducing agent via a disproportionation reaction (Equation 1.2) that produces a Cu(II) β-diketonate as a volatile by-product (L is a neutral donor ligand).

$$2(hfac)Cu^{(I)}(L) \rightarrow Cu(s) + Cu(hfac)_2(g) + 2L(g) \qquad \text{(Equation 1.2)}$$
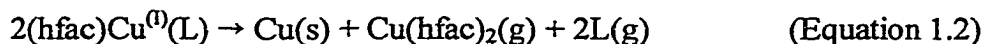
Van Hemert et al. first reported the use of $Cu(hfac)_2 \cdot H_2O$ as a Cu CVD precursor in 1965.[1.12] A film was deposited on a heated substrate in a warm wall, horizontal tube reactor, using H_2 at atmospheric pressure as the carrier and reducing gas. $Cu(hfac)_2 \cdot H_2O$ could be evaporated into the carrier gas stream at 90 °C with a substrate temperature of
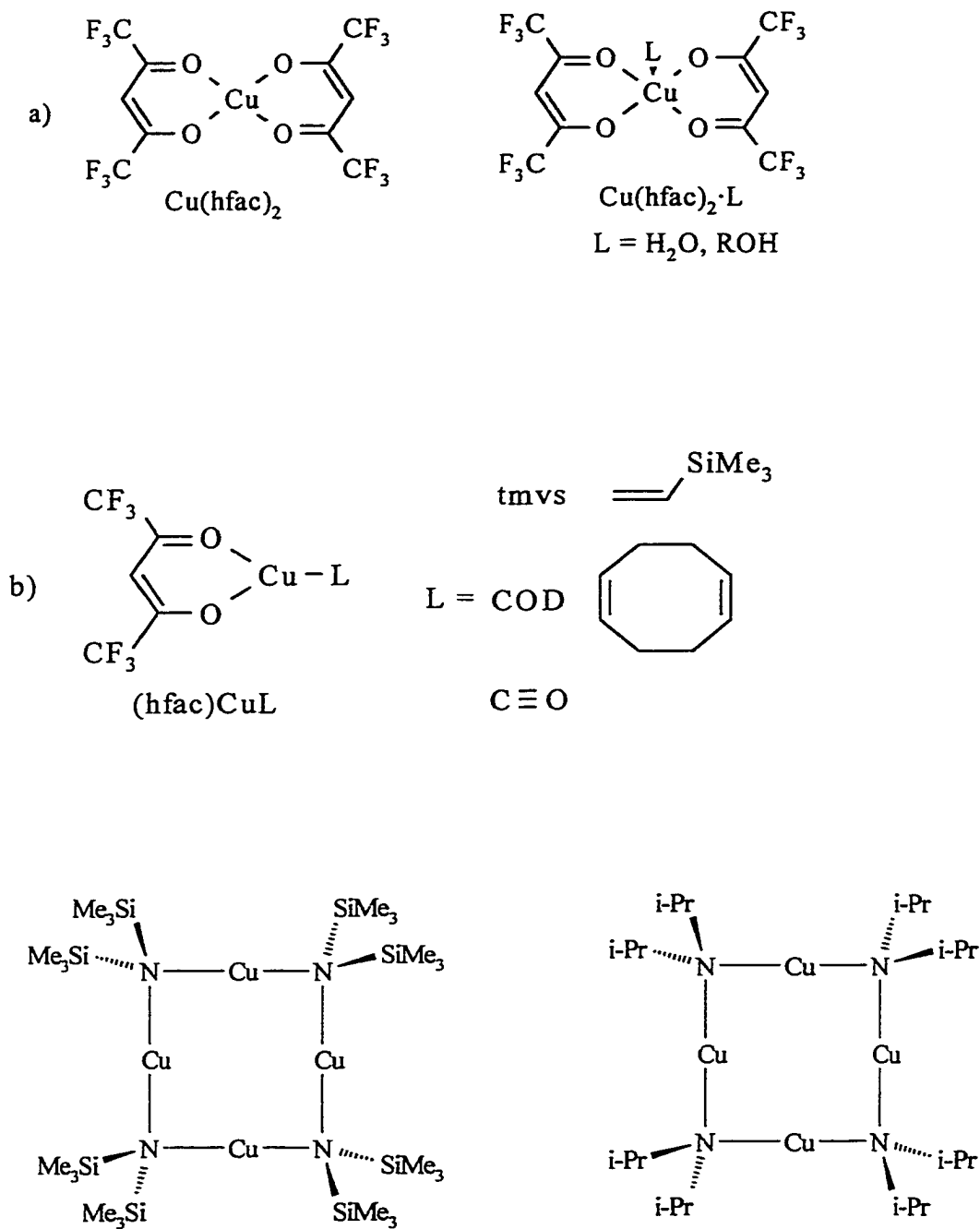
Figure 1.2 : Precursors for Chemical Vapor Deposition. a) Cu(II) b)Cu(I)

250 °C, to give high-quality films. Moshier et al. later reported a quantitative value of

80 nm/min for the deposition rate at 300 °C using $Cu(hfac)_2 \cdot H_2O$.[1.13]

Kaloyeros et al. were the first to report film resistivities that approach the value of

bulk copper using the reduction of $Cu(hfac)_2$ in H_2 carrier gas; they obtained resistivities

below 2.0 $\mu\Omega \cdot$cm for films deposited at temperatures as low as 250 °C.[1.14] Film growth

rates were 4-180 nm/min, depending upon the deposition conditions and the reactor

design. Within the past 10 years, the best CVD results for Cu(II) precursors were

obtained using $Cu(hfac)_2$ under hydrogen gas. However, several groups discovered that

film growth rates were enhanced with the use of Lewis base donors such as H_2O and

alcohols. Fluorinated β-diketonate ligands are strongly electron-withdrawing and

decrease the electron density on the metal center. This increases the ability of the copper

atom to coordinate a solvent molecule. It has been suggested that the liberated protons

from the additive (either H_2O or alcohols) enhance the reduction of Cu(II) to copper

metal from $Cu(hfac)_2$ by increasing the amount of protons available in the CVD process.

1.6 Photochemical Vapor Deposition

Photochemical Vapor Deposition is a process that uses a laser or some other light

source to excite a specific electronic excitation in the reactant, which activates the

molecule for a subsequent chemical reaction.[1.16] In a photochemical process, deposition

from the precursor excited state is more favorable than from its ground state, making the

reaction occur faster or at a lower temperature. Various types of light sources have been

used in the process such as Hg arc lamps, frequency doubled Ar ion lasers, and ArF and

KrF excimer lasers.[1.16]

Copper metal films have been deposited using Cu(hfac)$_2$·EtOH using UV photolysis.[1.15] Although films deposited by conventional CVD using this precursor were generally pure and crystalline, the photolytically deposited films were contaminated. X-ray photoelectron spectroscopy (XPS) and scanning Auger measurements showed that the films contained up to 50% carbon.[1.16] These films were contaminated because of fragmentation of the complex induced by the high-energy light sources used. However, if a photosensitive complex could be made that has a well defined excited state, then a minimal amount of energy necessary for the reduction to Cu metal will be applied. This will produce by-products that are stable and volatile that would not contaminate the Cu films.

This dissertation describes aspects of research into copper CVD. It discusses the use of photosensitive Cu(I) complexes as potential photoinduced deposition precursors. Our goal is to develop a new class of copper(I) precursors that are outside the (hfac)Cu(I) family. These precursors are important for two reasons: a) If the new precursors contain no O or F atoms, they may be useful for co-deposition of Cu-Al alloys. Cu films containing small amounts of Al are harder than pure Cu, with resistivity nearly as low as pure Cu metal. In order for these two metals to be deposited simultaneously, the Cu and Al CVD precursors must be compatible with each other. Because Al precursors are sensitive to O and F, Cu(hfac) precursors are not acceptable. b) New Cu(I) precursors may have readily accessible excited states for photochemical deposition reactions. The photochemistry of numerous Cu(I) complexes has been studied, but the photoactive species tend to be involatile because they are usually ionic salts.[1.17] A neutral,

photosensitive precursor could be used to develop a seed layer of Cu on the substrate, to enhance the selectivity of the overall deposition process.

We have examined tetrameric amide clusters i.e., $[CuN(SiMe_3)_2]_4$, $[CuNEt_2]_4$, $[CuN(i\text{-}Pr)_2]_4$, and $[CuN(t\text{-}Bu)(SiMe_3)]_4$; see structures in Figure 1.2. Each one of these precursors is phosphorescent and has the potential of being useful in photochemical deposition of Cu.

We also attempted to prepare lower nuclearity Cu(I) complexes derived from $[CuN(SiMe_3)_2]_4$. These complexes should be more volatile and still maintain photosensitivity. Although some promising results were obtained, isolation of well defined complexes was difficult due to their lability in solution.

1.7 Alcohol Adducts of $Cu(hfac)_2$ as Precursors

$Cu(hfac)_2$ is a versatile Lewis acid that can form adducts with various bases. Initially, hydrates, $Cu(hfac)_2 \cdot nH_2O$ (n = 1, 2) were studied.[1.18] Other adducts were reported in the literature such as $Cu(hfac)_2 \cdot pyridine$.[1.19] Although other adducts of $Cu(hfac)_2$ have been prepared, most experiments dealing with Cu CVD used the anhydrous compound or the hydrate.

In one of the first studies of the chemistry of $Cu(hfac)_2$ with other Lewis bases, Gafney and Lintvedt showed that UV irradiation of $Cu(hfac)_2$ in alcohol solutions led to the deposition of Cu metal.[1.20] In the 1990s, several groups demonstrated the importance of the addition of water and alcohols to $Cu(hfac)_2$ and how they improve deposition rates. Awaya and Arita showed that the addition of H_2O accelerated Cu film deposition.[1.21] Pilkington et al. also showed that $Cu(hfac)_2$-ROH mixtures (ROH = EtOH or a propanol isomer) could be used to produce Cu films under N_2 carrier gas at higher temperatures

(300–350 °C).[1.22] In some cases, excess water or alcohol was necessary for deposition to occur under N_2.

In kinetic studies of the deposition of Cu from $Cu(hfac)_2$ and H_2, Griffin and co-workers proposed that the rate determining step in the CVD process was the recombination of adsorbed hfac and H groups to form hfacH.[1.23] Therefore, the water or alcohol can serve as a source of H atoms to increase the concentration of H atoms adsorbed on the metal surface.[1.24] When H_2 is present, the H atoms it produces can recombine with the adsorbed $RO_{(ads)}$, making the overall role of ROH essentially catalytic.

My work has centered around alcohol adducts for their proton-transfer capabilities to produce Cu metal. It is possible that the alcohol molecules could reduce Cu(II) to Cu metal, thus making a reducing carrier gas (H_2) unnecessary for Cu CVD. This means that primary and secondary alcohols could liberate additional H atoms from the adsorbed alkoxy group to make either an aldehyde or ketone. Fan et al. studied $Cu(hfac)_2 \cdot i\text{-PrOH}$ as a self-reducing precursor under N_2 carrier gas. In these experiments, they were able to detect the carbonyl compound, i.e. acetone, from alcohol oxidation. However, in these experiments excess i-PrOH was needed to produce quality Cu films. Therefore, if a class of $Cu(hfac)_2$ adducts could be isolated that are volatile and stable to dissociation, then excess alcohol would be unnecessary. We have studied adducts with ethylene glycol (1), 2-methoxyethanol (2), propylene glycol (3), and 1-methoxy-2-propanol (4).

(1)　　　　(2)　　　　(3)　　　　(4)
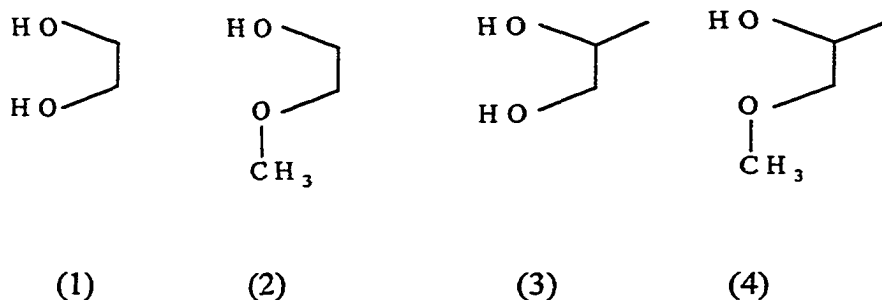
These ligands are capable of being bidentate. If the H atoms could be kept in close

proximity to the Cu(II) metal center, i.e. as stable Cu(hfac)$_2$ adducts, then deposition rates

could be enhanced by the readily available H atoms present. For an example, if

Cu(hfac)$_2$·1-methoxy-2-propanol was self-reducing, its Cu(II) could be reduced to Cu

metal and its 1-methoxy-2-propanol oxidized to methoxyacetone (Equation 1.3).
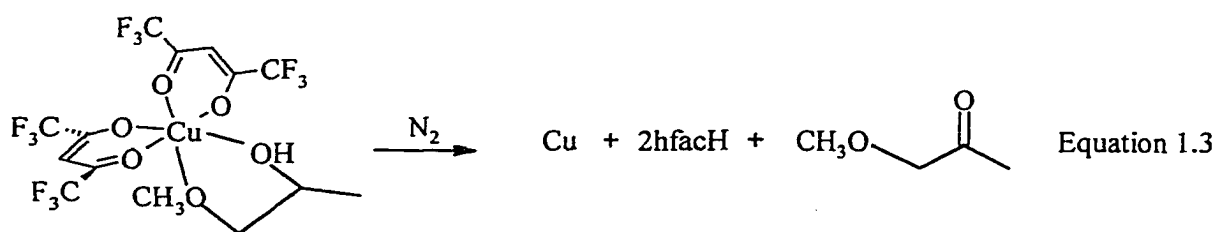
Therefore, a reducing gas and excess solvent would not be necessary for the reduction to

Cu metal in these complexes. We prepared adducts of Cu(hfac)$_2$ with all four of these

diols and ether-alcohols. The available evidence indicates that the new adducts are five-

coordinate (i.e. their structure is not as shown in Equation 1.3). However, the stability of

the complexes were improved compared to that of Cu(hfac)$_2$·i-PrOH. We were able to

deposit copper metal films under H$_2$. Under N$_2$ gas, no deposition occurred which means

that a reducing gas was necessary for Cu metal film production.

1.8 References

[1.1] Pierson, H. O. *Handbook of Chemical Vapor Deposition: Principles, Technology and Applications*; Noyes Publications: New Jersey, **1992**.

[1.2] Li, J.; Seidel, T. E.; Mayer, J. W. *MRS Bulletin*, **1994**, August, 15-18.

[1.3] Gelatos, A. V.; Jain, A.; Marsh, R.; Mogab, C. J. *MRS Bulletin*, **1994**, August, 49-54.

[1.4] Singer, P. *Semiconductor International*, **1994**, *17*(9), 57-64.

[1.5] Murarka, S. P. *Metallization Theory and Practice for VLSI and ULSI*; Butterworth-Heinemann, **1993**.

[1.6] Harper, J. M. E.; Colgan, E. G.; Hu, C-K; Hummel, J. P.; Buchwalter, L. P.; Uzoh, C. E. *MRS Bulletin*, **1994**, August, 23-29.

[1.7] Arita, Y.; Awaya, N.; Ohno, K.; Sato, M. *Tungsten and Other Advanced Metals for VLSI/ULSI Applications, 6th Proceedings Workshop*, **1989**, 335-344.

[1.8] Farkas, J.; Chi, K. M.; Kodas, T.; Hampden-Smith, M. *Advanced Metallization and Interconnect Systems for ULSI Applications*, **1995**.

[1.9] Norman, J. A. T.; Muratore, B. A.; Dyer, P. N.; Roberts, D. A.; Hochberg, A. K. *J. Phys. (Paris) IV*, **1991**, *1*(Coll. C2) p. 271.

[1.10] Polesnik, D. V.; Gilgen, H. H. "Laser-Controlled Etching of Semiconductors in Solutions"; in *Laser Chemical Processing for Microelectronics*; Ibbs, K. G.; Osgood, R. M., eds; Cambridge University Press, Cambridge, **1989**, 109-145.

[1.11] Kaanta, C. W.; Bausmith, R. C.; Cote, W. J.; Cronin, J. E.; Holland, K. L.; Lee, P. I. P; Wright, T. M. *Proc. IEEE, VMIC* Santa Clara, CA, 1991, p. 144.

[1.12] Van Hemert, R. L.; Spendlove, L. B.; Sievers, R. E. *J. Electrochem. Soc.*, **1965**, *112*, 1123-1126.

[1.13] Moshier, R. W.; Sievers, R. E. *Gas Chromatography of Metal Chelates*; Pergmon Press, Oxford, **1965**.

[1.14] Kaloyeros, A. E.; Feng, A.; Garhart, J.; Brooks, K. C.; Ghosh, S. K.; Saxena, A. N.; Luehrs, F. *J. Electron. Mater.*, **1990**, *19*, 271-273.

[1.15] Houle, F. A.; Baum, T. H.; Moylan, C. R. *Laser Chemical Processing for Microelectronics*; Ibbs, K. G.; Osgood, R. M., eds; Cambridge University Press, Cambridge, **1989**, 25-60.

[1.16] Jones, C. R.; Houle, F. A.; Kovac, C. A.; Baum, T. H. *Appl. Phys. Lett.* **1985**, *46*, p. 97.

[1.17] Kutal, C. *Coord. Chem. Rev.* **1990**, *99*, 213-252.

[1.18] Funck, L. L.; Ortolano, T. R. *Inorg. Chem.* **1968**, *7*, 567-573.

[1.19] Walker, W. R.; Li, N. C. *J. Inorg. Nucl. Chem.* **1970**, *9*, 47-52.

[1.20] Gafney, H. D.; Lintvedt, R. L. *J. Am. Chem. Soc.* **1971**, 93, 1623-1628.

[1.21] Awaya, N.; Arita, N. *Jpn. J. Appl. Phys.* **1993**, *32*(9A), 3915-3919.

[1.22] Pilkington, R. D.; Jones, P. A.; Ahmed, W.; Tomlinson, R. D.; Hill, A. E.; Smith, J. J.; Nuttal, R. *J. Phys. (Paris) IV*, **1991**, *1*(Coll. C2), 263-269.

[1.23] Lai, W. G.; Xie, Y.; Griffin, G. L. *J. Electrochem. Soc.* **1991**, *138*, 3499-3504.

[1.24] Bowker, M.; Madix, R. J. *Surf. Sci.* **1980**, *95*, 190-206.

Chapter 2

Phosphorescence and Structure of a Tetrameric Copper(I)-Amide Cluster

2.1 Introduction

Numerous volatile copper(I) complexes have been examined in recent years as possible precursors for the chemical vapor deposition (CVD) of copper metal.[2.1] The family of species (hfac)CuL (L = neutral ligand)[2.2] has been most intensively studied; other copper(I) precursors include $[CuOCMe_3]_4$[2.3] and $CpCuPEt_3$.[2.4]

We have been interested in volatile copper complexes that also show photochemical activity, so that Cu deposition might be induced by light.[2.5] Several studies of laser-induced Cu CVD have been reported.[2.6-2.11] However, these experiments have generally utilized high-energy laser sources, so that both photophysical (i.e. via laser-induced heating of the substrate) and photochemical processes have been observed. We wished to take advantage of copper(I) complexes that posses well defined low-energy excited states, which might react cleanly with reducing carrier gases to produce pure Cu. Although numerous copper(I) complexes are known to show photochemical activity,[2.12] many of these are ions (e.g. $Cu(Me_2phen)_2^+$, $Cu(phen)(PPh_3)_2^+$) whose salts have low volatility. In contrast, neutral metal amide complexes, especially those containing the bis(trimethylsilyl)amide ligand $((SiMe_3)_2N^-)$, are often distillable or sublimable.[2.13] We now report that the planar tetrameric copper(I) cluster $[CuN(SiMe_3)_2]_4$ (Figure 2.1) is both luminescent and sufficiently volatile for CVD of Cu films. Chisholm et al. have recently reported the use of $[CuN(SiMe_3)_2]_4$ as a precursor for Cu CVD.[2.14] However, their depositions were performed at 275 °C, whereas we show that Cu films form at substrate temperatures as low as 145 °C. In addition, we find a slightly lower threshold

$$Me_3Si\text{----}N\text{-----}Cu\text{-----}N\text{---}SiMe_3$$

(structure diagram with Me₃Si and SiMe₃ groups bonded to N atoms, connected through Cu atoms in a cluster)
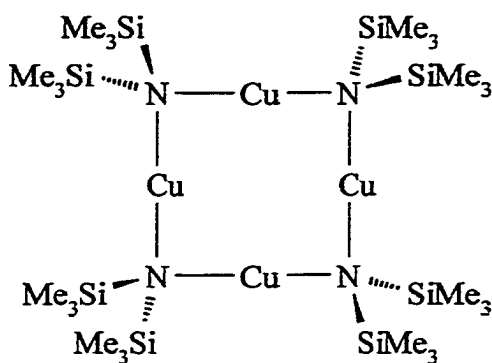
Figure 2.1 Sketch of [CuN(SiMe₃)₂]₄

temperature for Cu CVD with this precursor under Xe arc lamp irradiation.

Also reported here is the crystal structure of [CuN(SiMe₃)₂]₄. An X-ray analysis of the compound has been reported by Miele et al.[2.15] Our low-temperature data and lower-symmetry space group reveal a more precise and chemically more reasonable structure. An early X-ray study of the cluster, indicating its square-planar shape, was cited in 1980.[2.16] However, except for the Cu···Cu distances of 2.685 Å,[2.17] no details from that study appear to have been published.

2.2 Experimental

2.2.1 Materials and Procedures

Reagents were obtained from Aldrich Chemical Co. Solvents were HPLC or spectrophotometric grade and were used without further purification, except for tetrahydrofuran which was distilled from Na/benzophenone before use.

2.2.2 Preparation of [CuN(SiMe₃)₂]₄ from CuCl

A solution of NaN(SiMe₃)₂ (1 M; 5 mL) in THF was added dropwise to a suspension of CuCl (0.50 g; 5 mmol) in THF in a drybox, with stirring. After all of the sodium salt had been added, the mixture was stirred for 30 min, refluxed under N₂ for 1

h, evaporated to dryness, and the yellow-brown residue stirred with CH_2Cl_2-pentane (1:1 v/v; 40 mL). The resulting suspension was filtered to remove insoluble material and evaporated. If the residue was still colored, the extraction-filtration-evaporation procedure was repeated. Yield of colorless crystalline powder: 65-70%. NMR ($CDCl_3$, vs. TMS): ^1H, 0.35 ppm (200 MHz; lit.$^{2.18}$ 0.34 ppm); ^{13}C, 7.8 ppm (50 MHz). X-ray quality crystals of $[CuN(SiMe_3)_2]_4$ were grown over a period of several days by layering a THF solution of $LiN(SiMe_3)_2$ on a mixture of THF and CuCl.

2.2.3 Reactivity of $CuCl_2$ with $(SiMe_3)_2N^-$

Solid $LiN(SiMe_3)_2$ (1-2 equiv) was added to a suspension of anhydrous $CuCl_2$ in THF, causing the color to change quickly to purple. After the lithium salt had been added, the solvent was removed, at which point the color changed from purple to green. Attempts to isolate tractable copper(II) complexes from the purple and green materials failed, but if the solution was refluxed and allowed to cool, a solid containing $[CuN(SiMe_3)_2]_4$ precipitated.

2.2.4 Photophysical Data

Electronic absorption and corrected phosphorescence spectra were recorded by using Aviv Model 14DS and Spex Instruments Fluorolog 2 Model F112X (Hamamatsu R928 or R636 PMT) instruments, respectively with an excitation wavelength of 310 nm. An Oxford Instruments Model DN1704 cryostat was employed for low-temperature measurements. Lifetime measurements employed a Laser Photonics N_2 laser (337 nm, pulse width < 1 ns, energy 1 mJ) as excitation source, and colored-glass filters and a McPherson $\frac{1}{4}$-m monochromator to isolate the emitted light. The emission signal from the photomultiplier tube (Hamamatsu R928) was passed to a Hewlett-Packard model

54111D digitizing oscilloscope. Lifetimes were determined by exponential fits to the digitized phosphorescence decay curves, after subtraction of dark current.

2.2.5 X-ray Analysis

Diffraction data (Table 2.1) were collected on an Enraf-Nonius CAD4 diffractiometer fitted with Mo Kα source and graphite monochromator, using the θ-2θ scan method. Final unit cell constants were determined from the orientations of twenty-five centered high-angle reflections. The intensities were corrected for absorption using ψ scan data for five reflections. The crystal was cooled to 130 K in a thermostatted N_2 cold stream. The MOLEN[2.19] set of programs was used for structure solution and refinement. Atomic positions and selected distances and angles structure are in Table 2.2 and 2.3.

2.2.6 CVD Experiments

CVD experiments were performed under 1 atm H_2, with a flow rate of 100 mL min^{-1}. In initial experiments, the $[CuN(SiMe_3)_2]_4$ precursor was placed in a borosilicate glass tube inside a tube furnace, and H_2 was passed through the tube. For each CVD experiment using this apparatus, the furnace was warmed to a constant temperature while H_2 was passed over the precursor; passage of H_2 was continued for 30 min while the reactor was at temperature, and also during a subsequent cooling period (ca. 1 h).

To prepare Cu films suitable for analysis by X-ray powder diffraction, we also carried out deposition in a warm-wall pedestal reactor[2.20] with an upward-facing pedestal. For these experiments, because we anticipated that transporting the precursor from a separate flask to the substrate would be difficult, we placed the powdered solid precursor in the center of the substrate. Deposition then occurred on the substrate beneath and

Table 2.1 Crystal Data for [CuN(SiMe₃)₂]₄[a]

formula	$C_{24}H_{72}Cu_4Si_8N_4$
fw	895.7
space group	$P2/n$
Z	2
T/K	130
$\lambda/\text{Å}$	0.71073 (Mo Kα)
$a/\text{Å}$	9.285(3)
$b/\text{Å}$	13.393(3)
$c/\text{Å}$	17.752(5)
$\beta/°$	90.53(2)
$V/\text{Å}^3$	2208(2)
$\rho_x/\text{g cm}^{-3}$	1.347
μ/cm^{-1}	21.4
transm coeff	0.844-0.998
$R(F)$ (obs. data)[c]	0.061
$R_w(F)$[d]	0.041

[a]In Tables 2.1-2.3, estimated standard deviations in the least significant digits of the values are given in parentheses. [c]$R = \Sigma||F_o| - |F_c||/\Sigma|F_o|$; data with $I > 1\sigma(I)$. [d]$R_w = \sqrt{(\Sigma w(|F_o| - |F_c|)^2/\Sigma wF_o^2)}$; $w = 4F_o^2/(\sigma^2(I) + (0.02F_o^2)^2)$.

Table 2.2 Atomic Coordinates for $[CuN(SiMe_3)_2]_4$

	x	y	z	$U_{eq}/\text{Å}^2$ [a]
Cu1	0.29415(5)	0.34872(4)	0.17794(3)	0.0161(1)
Cu2	0.29474(5)	0.14884(4)	0.17821(3)	0.01496(9)
Si1	0.5255(1)	0.2554(1)	0.08604(5)	0.0189(2)
Si2	0.2202(1)	0.2396(1)	0.02694(6)	0.0204(2)
Si3	0.1017(1)	0.5185(1)	0.21481(7)	0.0243(3)
Si4	0.0942(1)	-0.02125(9)	0.22401(6)	0.0178(3)
N1	0.3389(3)	0.2483(3)	0.1042(1)	0.0152(6)
N2	¼	0.4506(3)	¼	0.016(1)
N3	¼	0.0461(4)	¼	0.018(1)
C1	0.6315(4)	0.2201(3)	0.1709(3)	0.026(1)
C2	0.5831(5)	0.1678(4)	0.0110(3)	0.040(1)
C3	0.5817(5)	0.3839(4)	0.0580(3)	0.032(1)
C4	0.0339(5)	0.2784(3)	0.0520(3)	0.029(1)
C5	0.2130(5)	0.1092(4)	-0.0096(3)	0.033(1)
C6	0.2731(5)	0.3227(4)	-0.0527(3)	0.037(1)
C7	0.0542(6)	0.6264(4)	0.2765(3)	0.044(1)
C8	-0.0640(5)	0.4408(4)	0.2102(3)	0.037(1)
C9	0.1360(5)	0.5654(4)	0.1177(3)	0.038(1)
C10	-0.0331(5)	0.0578(4)	0.1692(3)	0.027(1)
C11	-0.0042(5)	-0.0691(4)	0.3078(3)	0.028(1)
C12	0.1376(5)	-0.1296(3)	0.1613(3)	0.027(1)

$^a U_{eq} = \frac{1}{3}[a^2 a^{*2} U_{11} + b^2 b^{*2} U_{22} + c^2 c^{*2} U_{33} + 2aca^*c^*U_{13}\cos\beta]$.

Table 2.3 Selected Interatomic Distances/Å and Angles/° for $[CuN(SiMe_3)_2]_4$ at 130 K[a]

Cu1···Cu1´	2.6937(7)	Cu2···Cu2´	2.6883(7)	Si2-N1	1.756(3)
Cu1···Cu2	2.6670(7)	Cu2-N1	1.917(4)	Si3-N2	1.760(3)
Cu1-N1	1.925(4)	Cu2-N3	1.924(3)	Si4-N3	1.763(3)
Cu1-N2	1.917(3)	Si1-N1	1.768(3)	Si-C	1.853-1.875

N1-Cu1-N2	179.0(1)	Cu2-N1-Si2	110.6(2)	Si3-N2-Si3´	117.7(3)
N1-Cu2-N3	178.3(1)	Si1-N1-Si2	118.0(1)	Cu2-N3-Cu2´	88.7(2)
Cu1-N1-Cu2	88.3(1)	Cu1-N2-Cu1´	89.3(2)	Cu2-N3-Si4	111.99(6)
Cu1-N1-Si1	107.7(2)	Cu1-N2-Si3	107.61(6)	Cu-N3-Si4	110.96(6)
Cu1-N1-Si2	116.12(2)	Cu1-N2-Si3	115.69(6)	Si4-N3-Si4	118.4(3)
Cu2-N1-Si1	112.3(2)	Cu1-N2-Si3	107.61(6)		

[a]Primes refer to atoms related by the symmetry operation ½-x, y, ½-z.

around the precursor. The films were analyzed by using a Siemens automated powder diffractometer. Photoinduced depositions were carried out with the same apparaturs, but with the beam from a Kratos/Schoeffel 150-W Xe arc lamp focused through the Pyrex housing ($\lambda > 300$ nm) onto the substrate. The surface temperature of the substrate was monitored during the photochemical experiments to insure that there was no significant rise in temperature caused by the arc lamp.

2.3 Results

2.3.1 Synthesis and Properties

The tetranuclear copper(I) cluster $[CuN(SiMe_3)_2]_4$ studied here is a colorless, crystalline compound first reported by Bürger and Wannagat in 1964.[2.18] It is stable in air in the solid state for weeks, discoloring to pale blue over longer periods. The cluster is soluble in solvents such as CH_2Cl_2, ether, and THF, and sparingly soluble in pentane. These solutions are somewhat air-sensitive, but they can be prepared in air without significant decomposition if they are degassed (e.g. by bubbling with N_2) soon after preparation.

CuI and $CuCl_2$ were used as starting materials in the original preparation of the cluster.[2.18] We found that CuCl is also a satisfactory starting material. In addition, we were interested in the reactivity of copper(II) with $(SiMe_3)_2N^-$: if "$Cu^IN(SiMe_3)_2$" tetramerizes to make the $[CuN(SiMe_3)_2]_4$ cluster primarily in order to achieve a higher coordination number about Cu, then perhaps a mononuclear, and therefore more volatile, $Cu^{II}(N(SiMe_3)_2)_2$ complex would be isolable. In our experiments, adding $LiN(SiMe_3)_2$ to a suspension of $CuCl_2$ in THF led to the formation of a dark purple color. Since many copper(II) complexes with nitrogen coordination are purple, we thought this color might

be due to a Cu(II)-N(SiMe₃)₂ complex. However, we were unable to isolate any well-behaved Cu(II) complex from these solutions; instead, like the original authors, we found that they contained some of the copper(I) cluster [CuN(SiMe₃)₂]₄.

2.3.2 Structure of the cluster

[CuN(SiMe₃)₂]₄ contains an approximately square Cu_4N_4 core, with the Cu atoms at the centers of the sides, and N atoms of the N(SiMe₃)₂ groups at the corners. The symmetry of the $Cu_4N_4Si_8$ portion of the cluster is approximately D_{4h}; the Cu_4N_4 core of the cluster is planar within 0.007 Å. An ORTEP[2.21] drawing of the molecule appears in Figure 2.2.

Figure 2.2 shows a slight twisting of the trimethylsilyl groups away from the orientations of highest possible symmetry. At each N atom, if the two Me₃Si groups were perfectly staggered with respect to the other substituents, there would be close nonbonded contacts between two pairs of methyl groups. These close contacts include C2···C5 and C3···C6, as well as between C7, C9, C11, C12 and their symmetry-related counterparts C7', C9', C11', and C12'. Indeed, in the previously reported structure analysis of [CuN(SiMe₃)₂]₄,[2.15] where the molecular symmetry was required to be C_{2h}, the mirror plane imposed a requirement of an essentially perfectly eclipsed conformation on the methyl groups at Si1 and Si2, and constrained the conformation of the other methyl groups as well. One result of these requirements was close contacts between nonbonded C atoms (3.308 and 3.343 Å). However, in the present determination, the molecule has only twofold symmetry. This allows the SiMe₃ groups to twist slightly, so that the shortest intramolecular contact of this type is now C7···C9' (3.518 Å). The amount of twisting in the SiMe₃ groups is approximately 20°, as
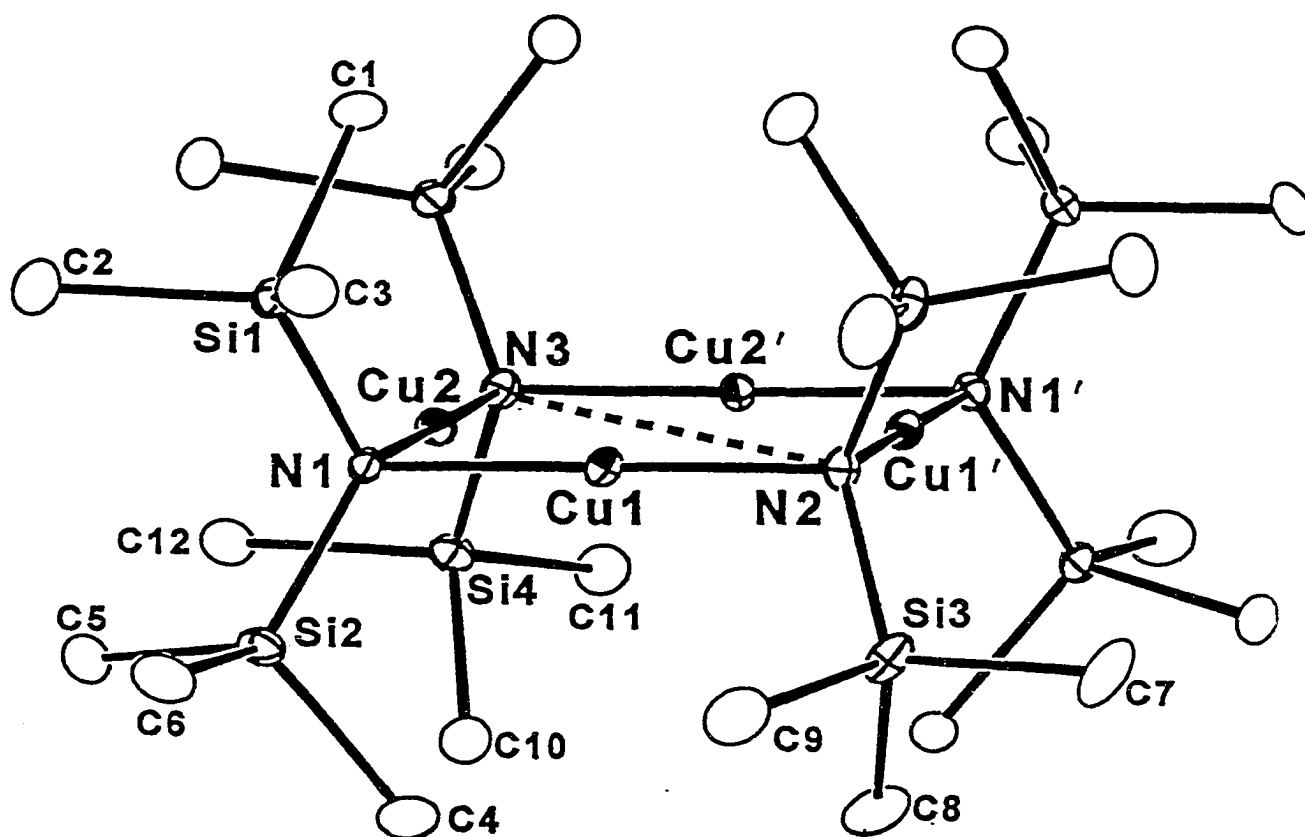
Figure 2.2 ORTEP[2.21] drawing of [CuN(SiMe₃)₂]₄ from 130 K data, with thermal
ellipsoids at the 50% probability level. H atoms omitted for clarity. Dashed
line shows crystallographically imposed twofold axis.

illustrated by the following torsion angles in our structure: C1-Si1-N1-Si2, −160.3(3)°; C4-Si2-N1-Si1, −159.4(3)°; C8-Si3-N2-Si3′, −160.9(3)°; C10-Si4-N3-Si4′, −160.8(3)°. The corresponding torsion angles in the previous X-ray analysis[2.15] are 180°, 180°, 178.6°, and −178.6°; the last two of these angles are required to have opposite signs because the two $N(SiMe_3)_2$ groups centered at N2 and N3 in $P2/n$ are related by the mirror plane in $I2/m$. The twisting does not constitute a large deviation from staggered conformations at the Si-N bonds, yet it reduces the unfavorable C···C interactions. All of the $SiMe_3$ groups in the molecule shown in Figure 2.2 are twisted in the same direction away from perfect staggering in our model: anticlockwise, when viewed looking toward the Cu_4N_4 core. Thus, the molecular symmetry is approximately D_4, in contrast to the approximate D_{4h} ($4/mmm$) symmetry of the Cu_4N_4 core. The $SiMe_3$ groups in the other molecule in the unit cell, the mirror image of the one illustrated in Figure 2.2, are twisted in the opposite direction. The higher-symmetry $I2/m$ model, in order to give molecular C_{2h} symmetry, requires either all fully staggered conformations or disorder between groups twisted clockwise and anticlockwise. If our model were superimposed on its mirror image, two sets of C atom positions would result; modeling them with a single set of C atoms with C_{2h} molecular symmetry would lead to large displacement parameters. This is exactly what was reported by Miele et al.[2.15] their U_{eq} values for the Cu, N, and Si atoms are very similar to ours, but for the C atoms they are 2-3 times as large. In summary, the present leads to a significantly more reasonable chemical picture for the molecule, especially in terms of intramolecular nonbonded contacts.

2.3.4 Electronic Spectra

Electronic absorption and emission spectra for $[CuN(SiMe_3)_2]_4$ are shown in Figure 2.3. The cluster is colorless, though it turns pale blue on prolonged exposure to air, probably due to partial oxidation to copper(II). The first two absorption maxima are those shown in Figure 2.3, at 283 (ε 1.65 x 10^4) and 246 nm (ε 1.7 x 10^4 M^{-1} cm^{-1}); no other bands are apparent at longer wavelengths even in more concentrated solutions. One of the most striking features of this cluster is its intense blue-green luminescence, which appears when the complex is excited at wavelengths below ca. 400 nm. Corrected emission spectra, also shown in Figure 2.3, are very similar for the solid and CH_2Cl_2 solution at room temperature and for the solid at 77 K. The corrected excitation spectrum in the 250-400 nm region for a dilute solution of the cluster is essentially identical to the absorption spectrum. The major difference observed at low temperature is that the emission band becomes narrower: fwhm 2400 cm^{-1}, vs. 3500 cm^{-1} at 300 K. Luminescence lifetimes can also be measured for the cluster by irradiation with a pulsed N_2 laser. Results of these measurements are summarized in Table 2.4. Two aspects of the data are of interest: first, in room-temperature solution, the lifetime is highly sensitive to the presence of O_2: and second, the lifetime is considerably longer at 77 K.

2.3.5 Chemical Vapor Deposition

The original report of the synthesis of $[CuN(SiMe_3)_2]_4$ describes its purification by sublimation at 180 °C and 0.2 Torr. Thus, it is much less volatile than the commonly used copper CVD precursors. (By comparison, $Cu(hfac)_2$ has a vapor pressure of
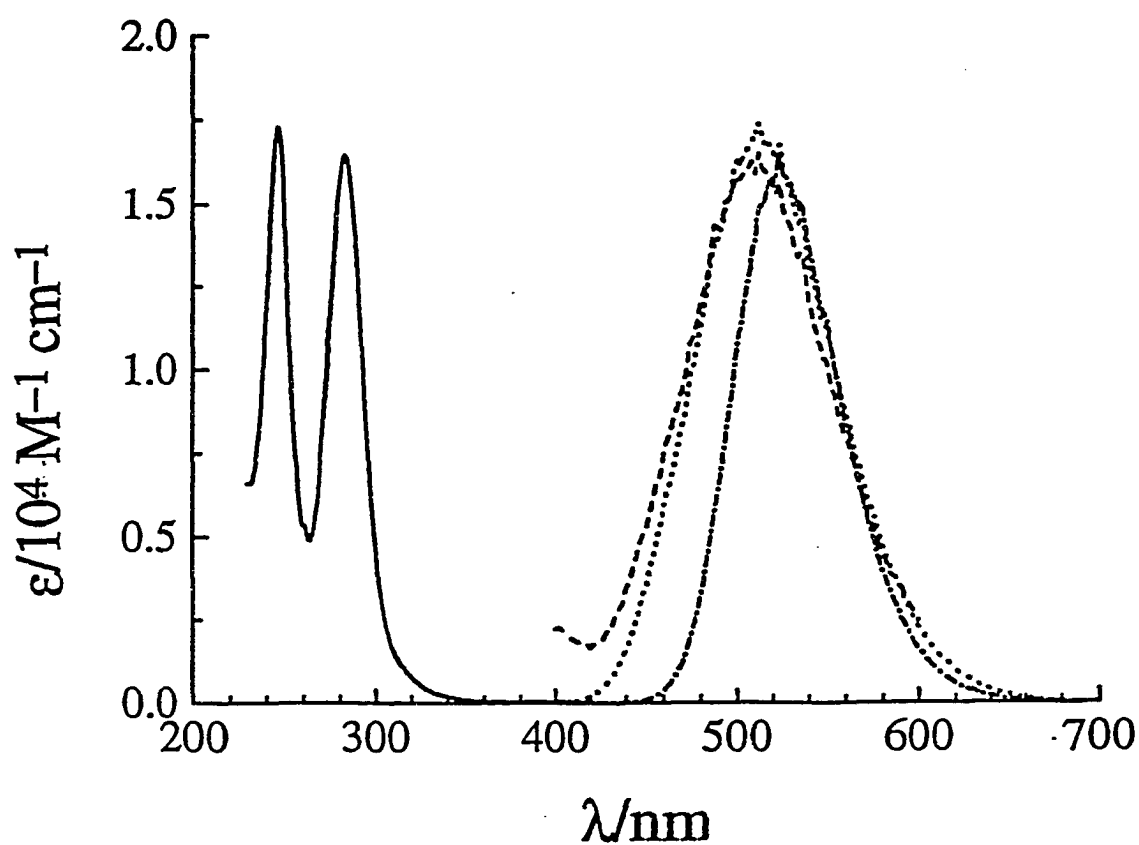
Figure 2.3 Electronic Spectra of [CuN(SiMe₃)₂]₄. Absorption: ——, 300 K, CH₂Cl₂
solution. Corrected phosphorescence (310 nm, excitation): -----, 300 K,
CH₂Cl₂ solution; ·······, 300 K, solid; --·--·--·, 77 K solid.

Table 2.4 Phosphorescence Lifetimes for $[CuN(SiMe_3)_2]_4$[a]

Medium	Temperature/K	Lifetime/μs
CH_2Cl_2 (aerated)	300	1.4
CH_2Cl_2 (degassed)	300	30
Solid	300	30
Et_2O (glass)	77	690

[a]±10%.

ca. 8 Torr at 100 °C.[2.22]) Nevertheless, the cluster's attractive photophysical properties

suggested that it might be useful in photochemical deposition of Cu. As a first step

toward such photochemical processes, we decided to determine whether $[CuN(SiMe_3)_2]_4$

can be used as a precursor for conventional (thermal) Cu CVD. In typical CVD

experiments,[2.1] the precursor is warmed in an evaporator, under a current of carrier gas,

and its vapor is then transported to the reactor, where the substrate is held at a higher

temperature to induce deposition. For example, when $Cu(hfac)_2$ is used as a CVD

precursor, it is usually evaporated at 70–100 °C, and Cu deposition occurs with H_2 carrier

gas at substrate temperatures of 200 °C and higher. However, in the present case, the low

volatility of $[CuN(SiMe_3)_2]_4$ meant that the required minimum temperature for

evaporation might be close to that for deposition; also, it was likely to be difficult to

transport the precursor vapor over long distances.

Initial experiments were performed with the precursor in a glass tube inside a tube

furnace. With this apparatus, we observed no changes in the precursor when the

temperature was kept at 160 °C or below. At 180 °C, some sublimed (but otherwise

unchanged) precursor could be observed on the cool tube walls at the downstream end of

the furnace. In contrast, treatment at 200 °C resulted in deposition of a Cu metal film near and downstream of the precursor. At these higher temperatures, some sublimation occurred as well, and after the deposition, the residual precursor showed some discoloration. At temperatures above 220 °C, decomposition of the precursor was extensive.

Cu films deposited as described above appeared metallic, but they were otherwise difficult to analyze. Therefore, we also carried out depositions in a warm-wall pedestal reactor, with the precursor placed directly onto the heated borosilicate glass or Si substrates. Deposition under H_2 at 200 °C (2.5 h) in this apparatus produced metallic films under and around the precursor that were 40-170 nm in thickness, as determined by stylus profilometry. These films were too thin for analysis by electrical (resistivity) methods. However, powder X-ray diffraction showed that the major component of the films was Cu, and that other possible crystalline phases (e.g. CuO, Cu_2O) were absent.

Deposition of Cu films was also observed with this apparatus at lower substrate/evaporation temperatures, although at lower rates: temperatures as low as 145 °C (H_2; 1 atm; 3 h) led to the formation of noticeable metallic Cu films when Si (with native oxide) was used as the substrate. These films formed only directly underneath the precursor, and although they were clearly metallic, they were too thin for analysis by other methods.

Experiments with photoinduced Cu deposition utilized the same apparatus and Si substrates, with the addition of a 150-W Xe arc lamp as light source. The deposition apparatus was made from borosilicate glass, restricting the light transmitted to the sample to wavelengths longer than ca. 300 nm. This, combined with the region of intense

absorptions of the cluster, namely below ca. 350 nm, indicates that the principal

irradiation wavelengths were in the 300-350 nm range under our conditions. When the

precursor was irradiated while being held at temperatures below 135 °C, some

discoloration occurred, but no Cu film deposition. However, at 136-138 °C (H_2; 1 atm; 3

h), a small amount of Cu film formed. Thus, the minimum substrate temperature for Cu

deposition with this precursor is slightly lower under near-UV irradiation than in the

dark.

2.4 Discussion

2.4.1 Structure of $[CuN(SiMe_3)_2]_4$ and related compounds

There are two common geometries for tetranuclear copper clusters. One is the

(approximately) planar $Cu_4(\mu\text{-}X)_4$ type reported herein. X-ray analyses have been

performed for a number of $Cu_4(\mu\text{-}X)_4$ clusters: $[CuNEt_2]_4$,[2.23] $[CuNMe_2]_4$ and several

other Cu(I) amide tetramers,[2.24] $[CuN(SiMe_2Ph)_2]_4$,[2.25] $[CuCH_2SiMe_3]_4$,[2.26] and

$[CuOCMe_3]_4$.[2.27] One other Cu(I) amide, $[CuN(SiMePh_2)_2]_3$, is a trigonal-planar

trimer,[2.25] likely because the trimeric structure minimizes repulsions between the

exceptionally bulky $N(SiMePh_2)_2$ groups. In most of the $Cu_4(\mu\text{-}X)_4$ structures, the Cu

and X atoms are approximately coplanar, but $[CuNEt_2]_4$[2.23] and $[CuN(SiMe_2Ph)_2]_4$[2.25]

have a distinct butterfly shape, with the Cu atoms approximately coplanar and the N

atoms alternating above and below this plane (Figure 2.4). Thus, the Cu_4N_4 core in the

"butterfly" clusters has approximate D_{2d} vs. D_{4h} in $[CuN(SiMe_3)_2]_4$.

The distances and angles in the Cu_4N_4 core of $[CuN(SiMe_3)_2]_4$ are similar to those

for the other amide tetramers. As Hope and Power observed for $[CuNEt_2]_4$,[2.23] the

distances in the amides are intermediate between those found for the Cu_4C_4 core of

Square-planar [Cu-μ-X]₄   "Butterfly" [Cu-μ-X]₄   "Cubane" [LCu-μ₃-X]₄
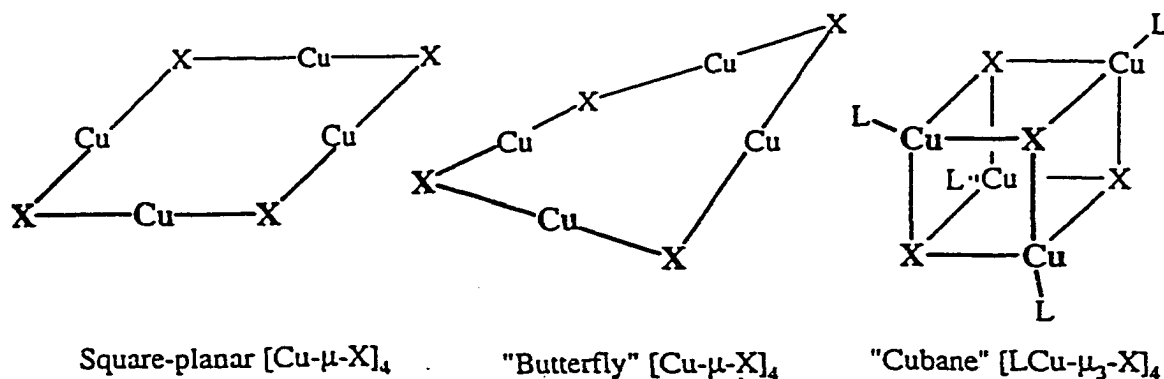
Figure 2.4 Illustrations of flat, butterfly and cubane structures

$[CuCH_2SiMe_3]_4$ (Cu-X longer, Cu···Cu shorter)[2.26] and for the Cu_4O_4 core of

$[CuOCMe_3]_4$ (Cu-X shorter, Cu···Cu longer).[2.27] This trend in Cu-X distances is expected

as a consequence of atomic size (O < N < C). The opposite trend in Cu···Cu, although

initially somewhat surprising, may reflect the increasing total coordination number at the

bridging X ligand in the order $[CuOCMe_3]_4$ (3) < $[CuNR_2]_4$ (4) < $[CuCH_2SiMe_3]_4$ (5).

The five-coordination at the bridging alkyl C atoms in $[CuCH_2SiMe_3]_4$, for example,

probably causes the smaller Cu-X-Cu angle, which in turn accommodates the larger Cu-

X distance and permits a closer Cu···Cu approach.

The other important family of Cu^I clusters is the "cubane" type, $[LCu-\mu_3-X]_4$, of

idealized symmetry T_d, in which the metal and triply bridging X occupy alternate corners

in a cube. For example, although $[CuOCMe_3]_4$ is square, as discussed above, its CO

adduct has the cubane-type structure, $[(OC)Cu-\mu_3-OCMe_3]_4$.[2.28] The cubane clusters are

structurally substantially different from the present compound, $[CuN(SiMe_3)_2]_4$, but they

are also of interest because several of them, including [LCuI]$_4$ (L = pyridine, piperidine) are photoactive.

2.4.2 Electronic Structure

Excited states of copper(I) complexes are of three types: interconfigurational, intraligand, and MLCT; the d^{10} configuration makes d-d and LMCT excited states impossible.[2.12] For [CuN(SiMe$_3$)$_2$]$_4$, low-energy intraligand transitions are unlikely: the lowest-energy electronic absorption band in hexamethyldisilazane, HN(SiMe$_3$)$_2$, is at 203 nm.[2.29] MLCT transitions cannot be conclusively ruled out, but the ligand LUMOs, probably the Si d orbitals, are likely to be at high energy. (Also, in the electronic spectrum of HN(SiMe$_3$)$_2$, the position of the first absorption maximum has been reported not to be highly solvent-sensitive.[2.29] This argues against an assignment involving charge transfer to Si.) Thus, the low-energy absorption and emission bands in this cluster are likely to be due to transitions primarily localized on the Cu atoms.

In simple mononuclear d^{10} complexes, interconfigurational transitions are commonly observed. For example, in the absorption spectra of monomeric M(PPh$_3$)$_3$ complexes (M = Pd, Pt), intense UV absorptions have been assigned to 3d$_{z^2}$ → 4p transitions.[2.30] However, in the present cluster, the Cu···Cu distances (ca. 2.7 Å; see Table 2.3) are less than twice the Cu van der Waals radius (1.43 Å[2.31]). Thus, it is likely that the cluster electronic states will involve substantial metal-metal interaction. Referring to the coordinate system in Figure 2.5, the Cu orbitals most likely to interact strongly with one another are the 3d$_{x^2-y^2}$ (filled) and 4s and 4p$_x$ (empty). These Cu atomic orbitals will combine to form three sets of MOs, each comprising a_{1g}, bonding; e_u, approximately nonbonding; and b_{1g}, antibonding (in idealized D_{4h} symmetry). The cluster LUMO is
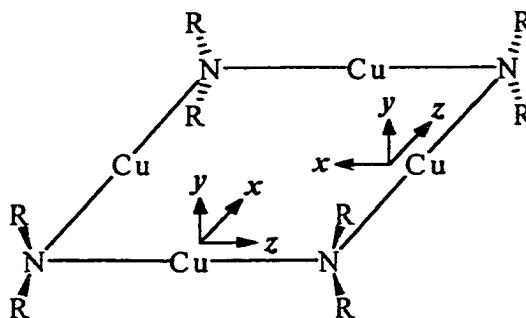
Figure 2.5 Coordinate systems for Cu atoms in [CuN(SiMe₃)₂]₄; SiMe₃ groups omitted for clarity. Cu p_x orbitals are expected to show maximum Cu···Cu interactions.

likely to be one of the a_{1g} combinations with a substantial contribution from Cu $4p_x$ AOs. (The HOMO may be a b_{1g} combination derived from $d_{x^2-y^2}$ AOs.)

The very long luminescence lifetime we observe for [CuN(SiMe₃)₂]₄ luminescence, 30 μs even in solution at room temperature, argues in favor of phosphorescence. The large Stokes shift between the emission and first absorption maxima in [CuN(SiMe₃)₂]₄ (ca. 15800 cm⁻¹ in CH₂Cl₂) may be due to a combination of two factors. First, if the lowest-energy excited state of the cluster involves population of an orbital with metal-metal bonding character, such as the empty $a_{1g}(4p_x)$ MO mentioned above, this could make the Cu···Cu distances significantly shorter in the excited state than in the ground state, leading to an unusually large Stokes shift. This behavior would be similar to that of the tetranuclear gold(I) clusters [Au(S₂CCH₃)]₄ and [AuCl(pip)]₄ (pip = piperidine): in these complexes, large Stokes shifts between absorption and emission have been attributed to substantial shortening of Au···Au distances in the excited state.[2-32] Second, if the HOMO is b_{1g}, as suggested above, then the lowest-energy spin-allowed

transition, $^1A_{1g} \rightarrow {}^1B_{1g}$ ($b_{1g}(3d_{x^2-y^2}) \rightarrow a_{1g}(4p_x)$) is electric-dipole-forbidden. This would make it weak and possibly difficult to observe in absorption. Then the first fully allowed transition, responsible for one of the intense absorptions in the UV, would be $^1A_{1g} \rightarrow {}^1E_u$ (e.g. $b_{1g}(3d_{x^2-y^2}) \rightarrow e_u(4p_x)$). These would be higher in energy than the HOMO–LUMO transition, increasing the Stokes shift still further.[2.33]

In addition to the polypyridine and phosphine species discussed in the Introduction, other examples of luminescent copper(I) complexes include the "cubane" clusters [(pip)CuI]$_4$ and [(py)CuI]$_4$ (py = pyridine).[2.34] Ford and co-workers have identified phosphorescent metal-centered (i.e. interconfigurational) excited states in both of these species, as well as an emissive interligand (I $\rightarrow$ py charge-transfer) state in the pyridine complex.[2.35] Phosphorescent copper(I) cluster ions containing phosphine and sulfur ligands have been reported recently, and their excited-state redox reactions studied.[2.36] Extended solids containing adducts of Cu(I) halides have been shown to be luminescent.[2.37] Interconfigurational phosphorescence has been observed from simple copper(I) species such as CuCl$_3{}^{2-}$ [2.38] and NaF:Cu$^+$.[2.39] Finally, a recent report describes an unusual example of *fluorescence* from a copper(I) complex, the bridged dimer Cu$_2$(PhNNNPh)$_2$.[2.30] (In this case, however, the triazenide ligands have extensive π systems, and the fluorescence appears to be primarily ligand-localized.)

The [CuN(SiMe$_3$)$_2$]$_4$ excited-state decay rate increases by about a factor of 20 in air-saturated solutions (see lifetimes in Table 2.4). This indicates efficient quenching of the cluster's phosphorescent excited state by O$_2$: the quenching rate constant is likely to be greater than 10^8 M^{-1} s^{-1}.[2.41] This is comparable to rate constants for reaction of excited Ru(bpy)$_3{}^{2+}$ with O$_2$: 6.8×10^8 M^{-1} s^{-1} in CHCl$_3$ [2.42] and 1.8×10^9 M^{-1} s^{-1} in CH$_3$OH.[2.43]

2.4.3 Deposition of Copper

The very low volatility of the [CuN(SiMe$_3$)$_2$]$_4$ cluster makes extensive CVD studies difficult, because the temperature required for significant vaporization of the compound (ca. 180 °C) is close to its decomposition temperature.

We observed two types of behavior at higher evaporation temperatures with this precursor under H$_2$ carrier gas. At ca. 180 °C, some evaporation occurred, as indicated by the collection of some white luminescent sublimate downstream from the heated zone; but no reduction to Cu occurred. At 200 °C, both precursor sublimation and Cu film deposition occurred. At the higher temperature the residual [CuN(SiMe$_3$)$_2$]$_4$ precursor also began to discolor during the deposition, to a yellowish-brown color. The Cu films that are produced under these conditions are not of high quality, but they are clearly metallic; some of the discoloration in the films, as well as their nonuniformity, may be due to the deposition geometry (i.e. evaporation and deposition areas in close proximity).

In order to determine whether the attractive photophysical properties of [CuN(SiMe$_3$)$_2$]$_4$ could be combined with the above CVD behavior, we carried out deposition experiments under Xe arc lamp irradiation, all under 1 atm H$_2$. With evaporation and deposition temperatures of 180 °C and higher, as outlined above, irradiation had no obvious effect on deposition rates. Therefore, we also performed experiments at lower temperatures. We discovered that small amounts (visible metallic films after 3 h) of Cu deposition occurred on Si substrates in the dark with evaporation/substrate temperatures as low as 145 °C. Due to the very low vapor pressure of the precursor at these temperatures, this deposition occurred only directly beneath the

solid precursor. This lower-temperature deposition process is slightly photosensitive: with Xe lamp irradiation, metallic films form at 136-138 °C.

Our best CVD results were obtained with Si substrates. This is similar to the work of Chisholm and co-workers,[2.14] who succeeded in depositing Cu films on Si (but not on quartz or glass) using $[CuN(SiMe_3)_2]_4$ as precursor. There are two differences between our work and the earlier one: First, we are able to use significantly lower substrate temperatures. This may be due to our use of H_2 as reducing carrier gas, as compared with the previous work, which was done at low pressure, without carrier gas. Second, we have demonstrated a small but measurable photochemical effect on our deposition process.

2.5 Conclusions

The square-planar tetrameric copper(I) cluster $[CuN(SiMe_3)_2]_4$ is intensely phosphorescent. The lifetime of this emission, which is likely to be associated with a metal-centered transition, is long and highly sensitive to the presence of dissolved O_2. Although the cluster has very low volatility, it is nevertheless possible to use it as a precursor in a simple CVD reactor for deposition of copper metal. Furthermore, this CVD process can be enhanced photochemically. Experiments now in progress include extending the chemical and photochemical vapor deposition experiments to other copper(I) amide clusters (for example, other Cu(I) amides,[2.44] as well as the cluster $[CuCH_2SiMe_3]_4$,[2.26] have been reported to be photosensitive), and chemical modifications that may lead to photophysically similar but monomeric (and thus more volatile) species.

2.6 References

[2.1] Hampden-Smith, M. J.; Kodas, T. T. In: *The Chemistry of Metal CVD*, Kodas, T. T.; Hampden-Smith, M. J., Eds.; VCH: Weinheim, 1994; ch. 5.

[2.2] Ligand abbreviations: hfacH = 1,1,1,5,5,5-hexafluoro-2,4-pentanedione; phen = 1,10-phenanthroline; Me$_2$phen = 2,9-dimethyl-1,10-phenanthroline; dppe = Ph$_2$PCH$_2$CH$_2$PPh$_2$.

[2.3] Jeffries, P. M.; Girolami, G. S. *Chem. Mater.* **1989**, *1*, 8-10.

[2.4] Beach, D. B.; LeGoues, F. K.; Hu, C.-K. *Chem. Mater.* **1990**, *2*, 216-219.

[2.5] For a discussion of applications and techniques of light-induced thin film deposition, see: Ibbs, K. G.; Osgood, R. M., Eds. *Laser Chemical Processing for Microelectronics*; Cambridge University Press: Cambridge, U. K., 1989.

[2.6] Dupuy, C. G.; Beach, D. B.; Hurst, J. E., Jr.; Jasinski, J. M. *Chem. Mater.* **1989**, *1*, 16-18.

[2.7] Jones, C. R.; Houle, F. A.; Kovac, C. A.; Baum, T. H. *Appl. Phys. Lett.* **1985**, *46*, 97. Wilson, R. J.; Houle, F. A. *Phys. Rev. Lett.* **1985**, *55*, 2184.

[2.8] Houle, F. A.; Wilson, R. J.; Baum, T. H. *J. Vac. Sci. Technol.* **1986**, *A4*, 2452.

[2.9] Markwalder, B.; Widmer, M.; Braichotte, D.; Van den Bergh, H. *J. Appl. Phys.* **1989**, *65*, 2470-2474.

[2.10] Han, J.; Jensen, K. F. *J. Appl. Phys.* **1994**, *75*, 2240-2250.

[2.11] Chen, Y. D.; Reisman, A.; Turlik, I.; Temple, D. *J. Electrochem. Soc.* **1995**, *142*, 3911-3918.

[2.12] Kutal, C. *Coord. Chem. Rev.* **1990**, *99*, 213-252.

[2.13] Lappert, M. F.; Power, P. P.; Sanger, A. R.; Srivastava, R. C. *Metal and Metalloid Amides*. Horwood: Chichester, England, 1980.

[2.14] Baxter, D. V.; Chisholm, M. H.; Gama, G. J.; Hector, A. L.; Parkin, I. P. *Advan. Mater.* **1995**, *7*, 49-51.

[2.15] Miele, P.; Foulon, J. D.; Hovnanian, N.; Durand, J.; Cot, L. *Eur. J. Solid State Inorg. Chem.* **1992**, *29*, 573-583.

[2.16] Hursthouse, M. B. Personal communication, in: Lappert, M. F.; Power, P. P.; Sanger, A. R.; Srivastava, R. C. *Metal and Metalloid Amides*. Horwood: Chichester, England, 1980; p. 493.

[2.17] Bradley, D. C. Unpublished work, cited in: ten Hoedt, R. W. M.; Noltes, J. G.; van Koten, G.; Spek, A. L. *J. Chem. Soc., Dalton Trans.* **1978**, 1800-1806.

[2.18] Bürger, H.; Wannagat, U. *Monatsh. Chem.* **1964**, *95*, 1099-1102.

[2.19] Fair, C. K. *MOLEN: An Interactive Structure Solution Procedure*; Enraf-Nonius: Delft, The Netherlands, 1990.

[2.20] This reactor is similar to one we have used previously (Kumar, R.; Fronczek, F. R.; Maverick, A. W.; Lai, W. G.; Griffin, G. L. *Chem. Mater.* **1992**, *4*, 577-582), except that its susceptor is 2.5 cm in diameter.

[2.21] Johnson, C. K. *ORTEP-II: A Fortran Thermal-Ellipsoid Plot Program for Crystal-Structure Illustrations*, Report ORNL-5138; National Technical Information Service, U. S. Department of Commerce: Springfield, VA, 1976.

[2.22] Temple, D.; Reisman, A. H. *J. Electrochem. Soc.* **1989**, *136*, 3525-3529. Wolf, W. R.; Sievers, R. E.; Brown, G. H. *Inorg. Chem.* **1972**, *11*, 1995-2002.

[2.23] Hope, H.; Power, P. *Inorg. Chem.* **1984**, *23*, 936-937.

[2.24] Gambarotta, S.; Bracci, M.; Floriani, C.; Chiesi-Villa, A.; Guastini, C. *J. Chem. Soc., Dalton Trans.* **1987**, 1883-1888.

[2.25] Chen, H.; Olmstead, M. M.; Shoner, S. C.; Power, P. P. *J. Chem. Soc., Dalton Trans.* **1992**, 451-457.

[2.26] (a) Jarvis, J. A. J.; Kilbourn, B. T.; Pearce, R.; Lappert, M. F. *J. Chem. Soc., Chem. Commun.* **1973**, 475-576. (b) Jarvis, J. A. J.; Pearce, R.; Lappert, M. F. *J. Chem. Soc., Dalton Trans.* **1977**, 999-1003.

[2.27] Greiser, T.; Weiss, E. *Chem. Ber.* **1976**, *109*, 3142-3146.

[2.28] Geerts, R. L.; Huffman, J. C.; Folting, K.; Lemmen, T. H.; Caulton, K. G. *J. Am. Chem. Soc.* **1983**, *105*, 3503-3506.

[2.29] Pitt, C. G.; Fowler, M. S. *J. Am. Chem. Soc.* **1967**, *89*, 6792-6793. Kirichenko, É. A.; Ermakov, A. I.; Pimkin, N. I.; Andrianov, K. A.; Kopylov, V. M.; Shkol'nik, M. I. *J. Gen. Chem. USSR* **1979**, *49*, 1333-1336.

[2.30] Harvey, P. D.; Gray, H. B. *J. Am. Chem. Soc.* **1988**, *110*, 2145-2147.

[2.31] Porterfield, W. W. *Inorganic Chemistry: A Unified Approach*; 2nd Ed.; Academic Press: New York, 1993; p. 214.

[2.32] Vogler, A.; Kunkely, H. *Chem. Phys. Lett.* **1988**, *150*, 135-137.

[2.33] If the prominent absorption and emission bands are associated with different electronic transitions, we might expect to find some evidence in the cluster's absorption spectrum (300-500 nm) for the spin-allowed partner of the phosphorescence transition. We found no such evidence, even in more concentrated solutions, although these experiments were limited somewhat by the low solubility of the cluster in common solvents.

[2.34] Vogler, A.; Kunkely, H. *J. Am. Chem. Soc.* **1986**, *108*, 7211-7212.

[2.35] Vitale, M.; Palke, W. E.; Ford, P. C. *J. Phys. Chem.* **1992**, *96*, 8329-8336. See also: Kyle, K. R.; Ryu, C. K.; DiBenedetto, J. A.; Ford, P. C. *J. Am. Chem. Soc.* **1991**, *113*, 5132-5137.

[2.36] Yam, V. W.-W.; Lee, W.-K.; Lai, T.-F. *J. Chem. Soc., Chem. Commun.* **1993**, 1571-1573.

[2.37] Rath, N. P.; Holt, E. M.; Tanimura, K. *Inorg. Chem.* **1985**, *24*, 3934-3938. Rath, N. P.; Holt, E. M.; Tanimura, K. *J. Chem. Soc., Dalton Trans.* **1986**, 2303-2310. Jasinski, J. P.; Rath, N. P.; Holt, E. M. *Inorg. Chim. Acta* **1985**, *97*, 91-97.

[2.38] Stevenson, K. L.; Braun, J. L.; Davis, D. D.; Kurtz, K. S.; Sparks, R. I. *Inorg. Chem.* **1988**, *27*, 3472-3476.

[2.39] Payne, S. A.; Goldberg, A. B.; McClure, D. S. *J. Chem. Phys.* **1983**, *78*, 3688-3697.

[2.40] Harvey, P. D. *Inorg. Chem.* **1995**, *34*, 2019-2024.

[2.41] We were unable to find data for the solubility of O_2 in CH_2Cl_2. We estimate a value of 0.008 M at 1 atm and 25 °C, based on data for $CHCl_3$ and CCl_4 tabulated in: Linke, W. F. *Solubilities of Inorganic and Metal-Organic Compounds*; v. 2; American Chemical Society, Washington, DC, 1965; p. 1234. This estimate leads to an O_2 quenching rate constant of $3 \times 10^8 \ M^{-1} \ s^{-1}$.

[2.42] Timpson, C. J.; Carter, C. C.; Olmsted, J., III *J. Phys. Chem.* **1989**, *93*, 4116-4120.

[2.43] Demas, J. N.; Harris, E. W.; McBride, R. P. *J. Am. Chem. Soc.* **1977**, *99*, 3547-3551.

[2.44] Yamamoto, T.; Ehara, Y.; Kubota, M.; Yamamoto, A. *Bull. Chem. Soc. Jpn.* **1980**, *53*, 1299-1302.

Chapter 3
Properties of Other Tetrameric Copper (I) Amide Clusters

3.1 Introduction

The research described in Chapter 2 concentrated on the tetrameric copper(I) amide cluster $[CuN(SiMe_3)_2]_4$.[3.1] It is less volatile than typical $Cu(hfac)_2$ and $Cu(hfac)L$ complexes but can be used as a CVD precursor. Since the temperature required for precursor evaporation and Cu metal deposition were similar, the solid precursor was placed on the substrate surface. Small amounts of Cu film formation were observed at temperatures as low as 145 °C.

We also studied the deposition using this precursor under UV irradiation. Under these conditions Cu deposition occurred at a slightly lower temperature, 136-138 °C, suggesting slight photochemical enhancement of the deposition process. This suggests that copper(I) amide complexes may be suitable precursors for both conventional and photoinduced CVD process. However, both the deposition rate for the non-photochemical process and the degree of enhancement under illumination need to be improved. Therefore, we have attempted to make more volatile Cu(I) complexes that still retain the $[Cu-NR_2]_n$ structure.

Taking into account the "$N(SiMe_3)_2$" ligand stabilizes low coordinate metal centers[3.2], we searched for ligands that would increase the volatility of the copper(I) amide clusters and still maintain photosensitivity. Hope and Power[3.3] synthesized a less bulky Cu(I) dialkylamide, $[CuNEt_2]_4$. What interested us about this complex was its reported sensitivity to light and the likelihood that its smaller amide group might make it more volatile than $[CuN(SiMe_3)_2]_4$. Therefore, we prepared $[CuNEt_2]_4$, and the two new

43

amide clusters [CuN(i-Pr)$_2$]$_4$ and [CuN(t-Bu)(SiMe$_3$)]$_4$, and studied them as potential

chemical and photochemical vapor deposition precursors (Figure 3.1).

3.2 Experimental

All manipulations were carried out in the dry box or under an inert atmosphere.

HNEt$_2$ was purified by distillation, purged with N$_2$, and stored in the dry box. LiN(i-Pr)$_2$

and HN(t-Bu)(SiMe$_3$) were purchased from Aldrich in sure seal bottles and stored in the

dry box.

3.2.1 Preparation of [CuNEt$_2$]$_4$[3.3]

A solution formed by the addition of 11.6 mL of a 1.6 M solution of n-

butyllithium in n-hexane to diethylamine (2.05 mL, 0.02 mol) in ether (10 mL) was

added dropwise to a well stirred slurry of copper(I) chloride (1.98 g, 0.02 mol) in ether

(20 mL) at −10 °C. The solution was protected from excessive light exposure by

aluminum foil. During the addition the slurry changed from lime green to brownish gray.

Stirring was continued for 4 hrs at −10 °C, and the solution was filtered through celite by

gravity filtration inside the dry box. A cloudy yellow solution was obtained; this was

refiltered through celite. The solution was evaporated from ca. 30 to 15 mL in vacuo. A

colorless precipitate was observed with a transparent yellow solution. The yellow

solution was discarded and the colorless precipitate was washed with pentane. Yield of

colorless powder: 60-65%. This complex exhibits pale yellow luminescence when

placed under a UV lamp.

3.2.2 Preparation of [CuN(t-Bu)(SiMe$_3$)]$_4$

[CuN(t-Bu)(SiMe$_3$)]$_4$ was prepared by an analogous from HN(t-butyl)(SiMe$_3$).

Yield of colorless powder: 55-57%.

Et Et

Et ·····,,, N —— Cu —— N Et

Cu Cu

Et N —— Cu —— N ·····. Et

Et Et

i-Pr i-Pr Me₃Si SiMe₃

i-Pr ·····,, N —— Cu —— N i-Pr t-Bu ·····,, N —— Cu —— N t-Bu

Cu Cu Cu Cu

i-Pr N —— Cu —— N ·····. i-Pr t-Bu N —— Cu —— N ·····. t-Bu

i-Pr i-Pr Me₃Si SiMe₃

(one possible isomer shown)
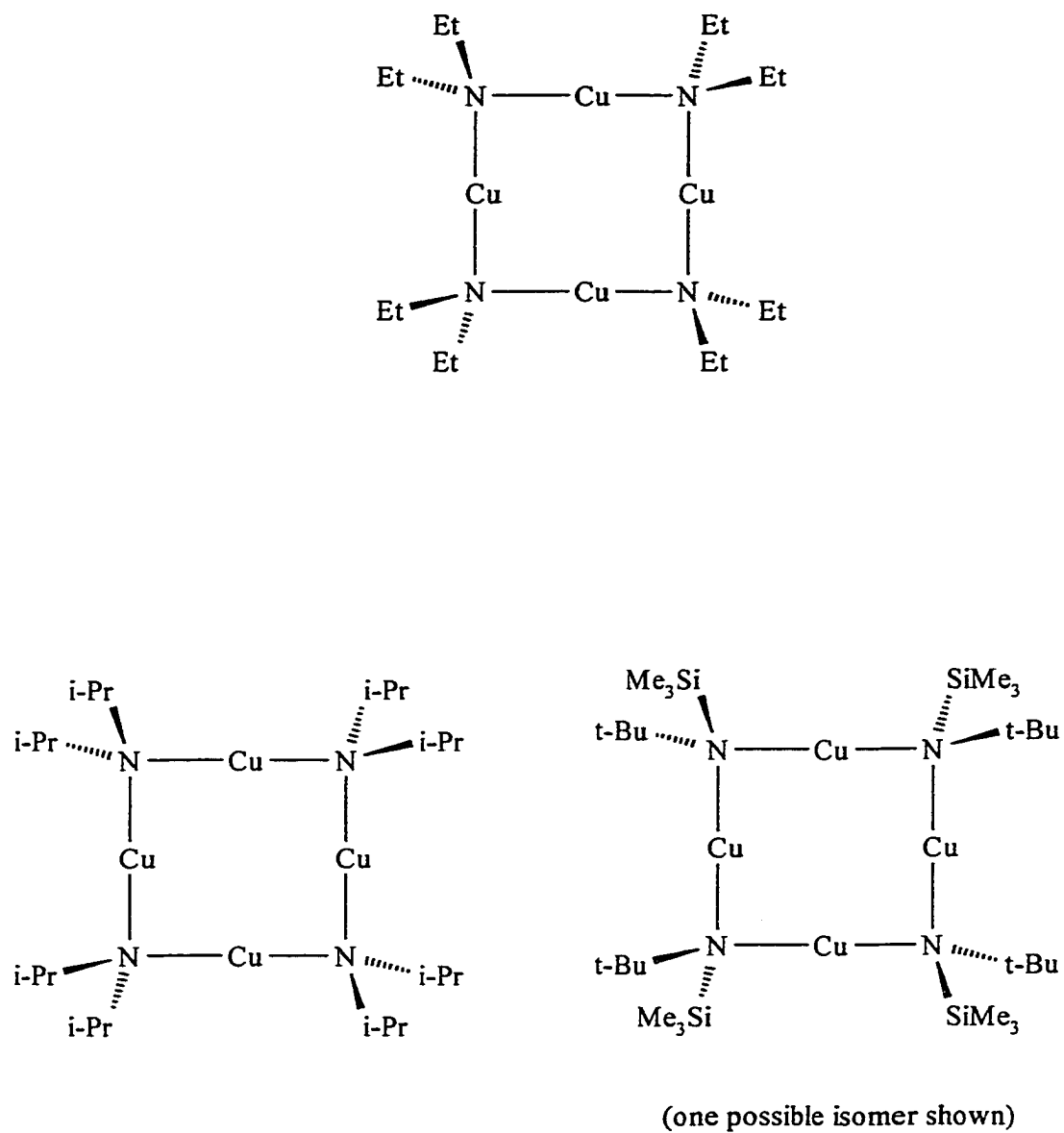
Figure 3.1 Tetrameric Copper(I) Clusters

3.2.3 Preparation of [CuN(i-Pr)$_2$]$_4$

CuCl (1.98 g 0.02 mol) was suspended in ether (20 mL). The round bottom was covered in aluminum foil to prevent excess exposure to light. The reaction mixture was assembled in the dry box. The slurry was cooled to −10 °C under N$_2$. LiN(i-Pr)$_2$·thf (4.39 mL, 0.02 mol) was added dropwise to the lime green slurry. During the addition the lime green solution changed from lime green to brownish gray. Stirring was continued for 4 hrs at −10 °C. The brownish gray solution was placed inside the dry box and filtered over celite by gravity filtration. A cloudy yellow solution was obtained. This was refiltered until a transparent yellow solution was obtained. The solution was evaporated from 30 mL to ca. 15 mL in vacuo, where upon a colorless precipitate was obtained and washed with pentane. Yield of colorless [CuN(i-Pr)$_2$]$_4$: 65-70%.

3.2.4 Photophysical Data

Phosphorescence spectra were recorded by using a Spex Instruments Fluorolog 2 Model F112X instrument and corrected for variations in PMT response with wavelength (Hamamatsu R928 or R636). Low temperature measurements were obtained by placing the clusters in NMR tubes and cooling them in liquid N$_2$.

3.2.5 CVD Experiments

CVD experiments were performed under 1 atm H$_2$, with a flow rate of 400 mL min^{-1} for 1 hr. A conventional CVD warm-wall pedestal reactor was used. In these experiments, the precursor is warmed in an evaporator, under a current of carrier gas, and its vapor is then transported to the reactor, where the substrate is held at a higher temperature to induce deposition. The [CuN(i-Pr)$_2$]$_4$ and [CuN(t-Bu)(SiMe$_3$)]$_4$ evaporation temperatures were between 135-140 °C and the substrate temperature was 200 °C.

3.3 Results

3.3.1 Synthesis and Properties

The tetranuclear clusters [CuNEt$_2$]$_4$, [CuN(i-Pr)$_2$]$_4$, and [CuN(t-Bu)(SiMe$_3$)]$_4$ studied are colorless, crystalline compounds. [CuNEt$_2$]$_4$ was first reported by Hope and Power.[3.3] These clusters are very sensitive to air: they change from colorless to yellowish-brown on exposure. They decompose in solution. [CuN(i-Pr)$_2$]$_4$ was characterized by FAB-MS in positive ion. FAB-MS: (Mass: 652, 653, 654, 655, 656, 657, 658); (Actual Abundance (%): 44, 19, 100, 36, 62, 13, 15); (Calculated Abundance (%): 55, 15, 100, 29, 69, 19, 22).

3.3.2 Electronic Spectra

The corrected solid state emission spectra are shown in Figures 3.1 and 3.2 for [CuN(i-Pr)$_2$]$_4$ and [CuN(t-Bu)(SiMe$_3$)]$_4$. Both complexes exhibit pale yellow luminescence at room and low temperature (77 K) in the solid state. The pale yellow luminescence appears when the complexes are excited at wavelengths below ca. 400 nm.

3.3.3 Chemical Vapor Deposition

Conventional CVD methods take into consideration the volatility of various compounds. For example, Cu(hfac)$_2$ has a vapor pressure of 8 Torr at 100 °C.[3.8] Nevertheless, the photophysical properties of these complexes suggest that they could be useful as photochemical precursors for copper metal deposition. We decided to determine whether [CuNEt$_2$]$_4$, [CuN(i-Pr)$_2$]$_4$ and [Cu(t-Bu)(SiMe$_3$)]$_4$ could be used as a precursor for conventional (thermal) Cu CVD. We assume that [CuNEt$_2$]$_4$, [CuN(i-Pr)$_2$]$_4$, and [CuN(t-Bu)(SiMe$_3$)]$_4$ would be more volatile than [CuN(SiMe$_3$)$_2$]$_4$ due to fact that
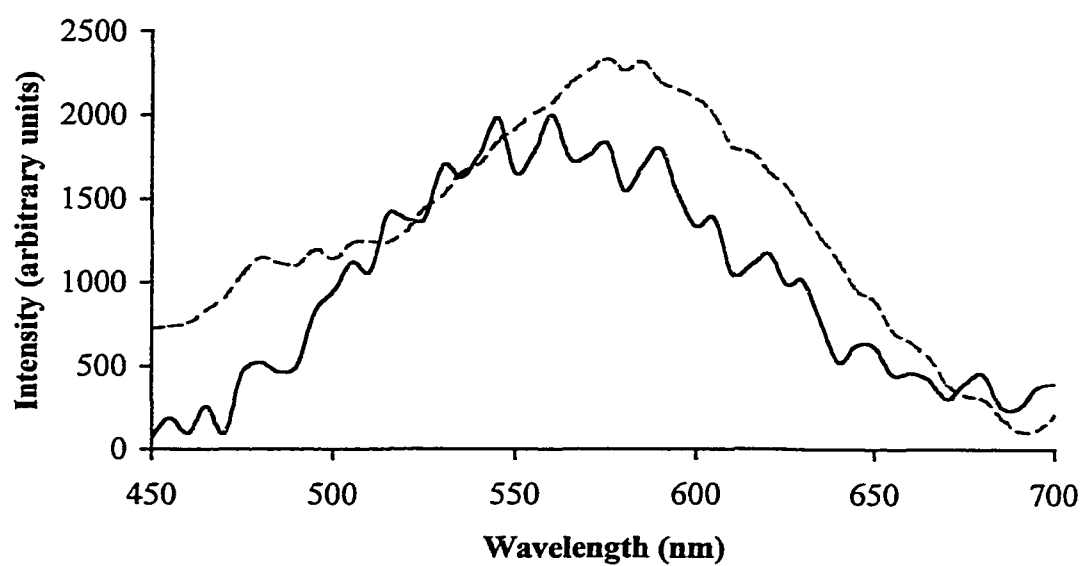
Figure 3.2 Solid State Emission Spectra of [CuN(i-Pr)$_2$]$_4$; ——, 300 K, solid; ------, 77 K, solid
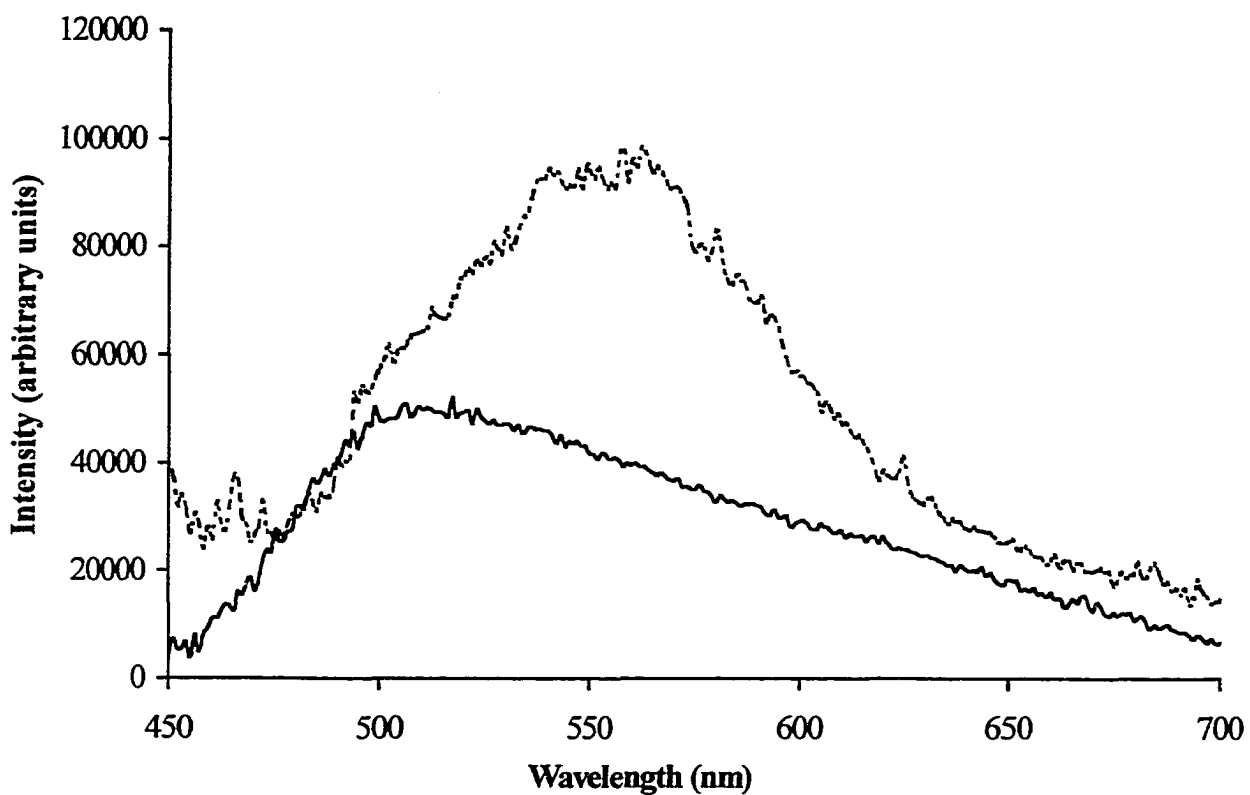
Figure 3.3 Solid State Emission Spectra of [CuN(t-Bu)(SiMe₃)]₄; ——, 300 K, solid; ------, 77 K, solid

other amide ligands are not as bulky as the bis(trimethylsilylamide) ligand. Preliminary results indicate that $[CuN(i-Pr)_2]_4$ and $[Cu(t-Bu)(SiMe_3)]_4$ decomposed when the substrate temperature was 200 °C and precursor temperatures at 135-140 °C. The precursors changed from colorless to brown with a hint of yellow.

3.4 Discussion

3.4.1 Deposition of Copper

Even though $[CuN(SiMe_3)_2]_4$ is low in volatility, Cu metal deposition was observed. However, there are some problems that can occur with compounds that are involatile. One of the problems is the transport of the precursor vapors over long distances. When a compound is involatile, it is very difficult to keep the temperature high enough so that the compound can remain in its vapor phase to be transported to the deposition area. Another problem for involatile compounds is the minimum required temperature for evaporation of the compound. If the evaporation temperature is too close to the deposition temperature than decomposition of the compound may occur before it reaches the substrate.

$[CuNEt_2]_4$, $[CuN(i-Pr)_2]_4$, and $[Cu(t-Bu)(SiMe_3)]_4$ are more air-sensitive than $[CuN(SiMe_3)_2]_4$. This made them difficult to work with in our conventional CVD reactor; we observed only decomposition of the precursors.

3.5 Conclusions

$[CuNEt_2]_4$, $[CuN(i-Pr)_2]_4$, and $[Cu(t-bu)(SiMe_3)]_4$ are tetramer clusters that exhibit pale yellow luminescence in the solid state. Thus, they have excited states that are similar to those of $[CuN(SiMe_3)_2]_4$. Therefore, they have the potential of being photochemical

vapor deposition precursors. Preliminary CVD experiments with these complexes have

been unsuccessful, probably because of rapid decomposition in the presence of traces of

O_2.

3.6 References

[3.1] James, A. M., Laxman, R., Fronczek, F. R., Maverick, A. W. *Inorg. Chem.*, **1998**, 37, 3785-3791.

[3.2] Lappert, M. F.; Power, P. P.; Sanger, A. R.; Srivastava, R. C. *Metals and Metalloid Amides: Synthesis, Structures, and Physical and Chemical Properties*, Ellis Horwood Series in Chemical Science, New York, **1980**.

[3.3] Hope, H., Power, P. P. *Inorg. Chem.*, **1984**, 936-937.

[3.4] Gambarotta, S., Bracci, M., Floriani, C., Chiesi-Villa, A., Guastini, C. *J. Chem. Soc. Dalton Trans.*, **1987**, 1883-1888.

[3.5] Lopes, C., Håkanasson, M., Jagner, S. *Inorg.Chem.*, **1997**, *36*, 3232-3236.

[3.6] Liaw, B., Orchard, S. W., Kutal, C. *Inorg. Chem.*, **1988**, *27*, 1311-1316.

[3.7] Ryu, C. K., Kyle, K. R., Ford, P. C. *Inorg. Chem.*, **1991**, *30*, 3982-3986.

[3.8] Temple, D.; Reisman, A. H. *J.Electrochem. Soc.* **1989**, *136*, 3525-3529. Wolf, W. R.; Sievers, R. E.; Brown, G. H. Inorg. Chem. **1972**, *11*, 1995-2002.

Chapter 4

Attempted Preparation of Lower Nuclearity Copper (I) Amides

4.1 Introduction

Although much work has been done with conventional (thermal) CVD, there has been considerable interest in precursors capable of photoinduced CVD. Luminescent complexes offer excited states which may be used to cause decomposition in a highly specific and controllable way. Our goal is to develop a new class of copper(I) precursors that are both volatile and light-sensitive.

The new class of compounds we are interested in making is metal amides, i.e. M-NR_2. These amides could be mono, bi-, oligo-, or polynuclear. This complexity arises because in the monomeric structure there is in principle both a donor (N) and an acceptor (M) site, and hence higher-nuclearity species can be derived from it by autocomplexation.[4.3] (Equation 4.1 and Scheme 4.1)

$$(Me_3Si)_2N^- + M^{n+} \rightarrow [MN(SiMe_3)_2]_m \qquad \text{Equation 4.1}$$
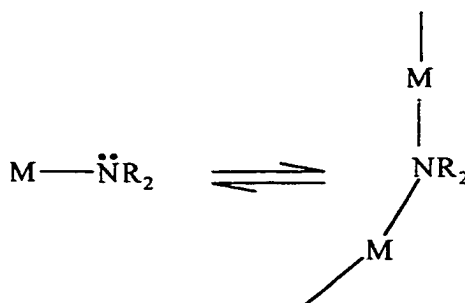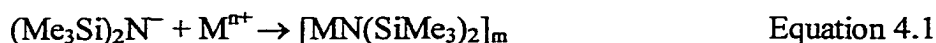
Scheme 4.1

A variety of low co-ordinate metal complexes have been prepared with the bis(trimethylsilyl)amide ligand. The significance of this ligand is due to a number of

52

factors: (a) the common ligand transfer reagents $LiN(SiMe_3)_2$ and $NaN(SiMe_3)_2$ are easily prepared; (b) the ligand is extremely bulky and often stabilizes metals in low-coordinate environments; (c) $d\pi$-$p\pi$ bonding may act as a contributing stabilizing factor for low coordinate metal centers; and (d) the metal complexes tend to be volatile.

Our work has centered around a tetrameric copper(I) amide cluster, $[CuN(SiMe_3)_2]_4$.[4,15] Despite the low volatility of this complex, it can be used as a precursor for chemical vapor deposition of copper metal with H_2 reducing gas, with both source and substrate at ca. 200 °C. Smaller amounts of Cu metal films are also deposited when the substrate temperature is as low as 150 °C (in the dark), or ca. 140 °C (under Pyrex-filtered Xe arc lamp illumination). Thus, this precursor shows slight photochemical enhancement. At 200 °C, deposition rates were higher, but still well below those for the $Cu(hfac)_2$ and its adducts.

We attempted to prepare monomeric $CuN(SiMe_3)_2$ complexes with neutral donor ligands L, (e.g. $L_nCuN(SiMe_3)_2$; L = CO, PR_3, CNR; n = 1-3) (Figure 4.1). We expected
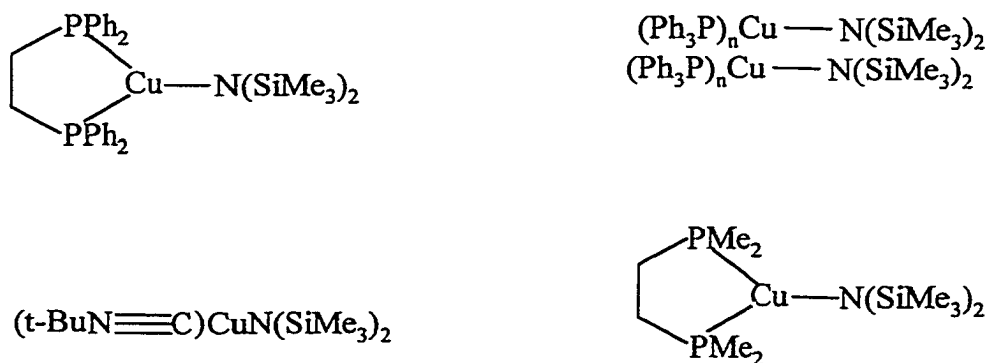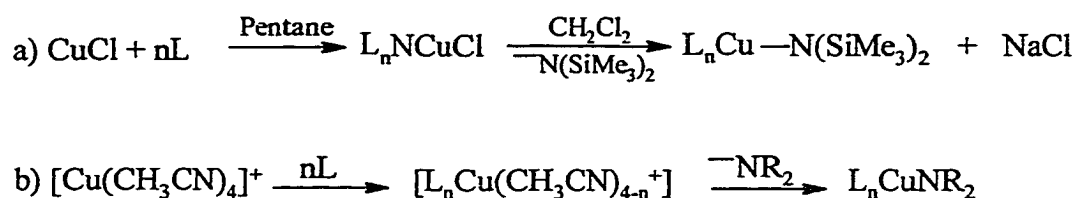

Figure 4.1 Target Monomeric Complexes $L_nCuN(SiMe_3)_2$

that these complexes would be more volatile than the copper cluster, $[CuN(SiMe_3)_2]_4$, and

still photosensitive. The synthesis of the mononuclear metal complexes, $L_nCuN(SiMe_3)_2$,

$L=$ phosphine or t-butyl isocyanide, was attempted by using CuCl and $[Cu(CH_3CN)_4]PF_6$

(Scheme 4.2). Some of the materials isolated in these experiments exhibit luminescence

in the solid state.

a) $CuCl + nL \xrightarrow{\text{Pentane}} L_nNCuCl \xrightarrow[\overline{}N(SiMe_3)_2]{CH_2Cl_2} L_nCu-N(SiMe_3)_2 + NaCl$

b) $[Cu(CH_3CN)_4]^+ \xrightarrow{nL} [L_nCu(CH_3CN)_{4-n}{}^+] \xrightarrow{\overline{}NR_2} L_nCuNR_2$

Scheme 4.2 Synthetic routes utilized in attempts to make L_nCuNR_2

$[Cu(CH_3CN)_4]PF_6$ is a promising route for monomeric Cu complexes because of

the ready dissociation of its acetonitrile ligands. The phosphine ligands that were tried

are dppe, dmpe, and dppm. We were only successful in the characterization of a side

product isolated in the reaction of $[Cu(CH_3CN)_4]PF_6$ with dppe,

$[Cu_2(dppe)(CH_3CN)_4](PF_6)_2$. Our difficulties in isolating well-defined complexes in

these reactions are likely due to the lability of the copper(I) systems.

4.2 Experimental

All reactions and manipulations were performed using standard dry-box

techniques. Reagents and solvents were obtained from Aldrich. Anhydrous solvents

were purchased in Sure Seal bottles and stored in a dry-box. PPh$_3$, dmpe, dppm and dppe

were obtained from Organometallics, Inc. The phosphines were free of phosphine

oxides, as determined by ^{31}P NMR. ^{1}H NMR and ^{31}P NMR spectra were obtained using a

Bruker AC 250 spectrometer. ^{31}P chemical shifts are reported in ppm downfield from 85% H_3PO_4, with triphenylphosphine as the internal reference.

Emission spectra were obtained by using a Spex Instruments Fluorolog 2 Model F112X fluorimeter, with Hamamatsu R928 or R636 PMT; they were corrected for variations in detector response with wavelength. FT-IR spectra were recorded as thin films on a Perkin-Elmer 1760 FT-IR spectrometer.

4.2.1 X-ray Analysis

Diffraction data (see summary in Table 4.3) were collected at 298 K on a Enraf-Nonius CAD4 diffractometer fitted with CuKα source and graphite monochromator, using the θ-2θ scan method. Final unit cell constants were determined from the orientations of twenty-five centered high-angle reflections. The intensities were corrected for absorption using ψ scan data for five reflections. The MOLEN set of programs was used for structure and refinement.

4.2.2 Attempted Preparation of $(Ph_3P)_nCuN(SiMe_3)_2$

Copper(I) chloride (0.99 g, 10 mmol) was suspended in 40 mL of pentane in a dry-box. After 5 minutes, PPh₃ (2.62 g, 10 mmol) was added to the suspension. The slurry started to change from a light lime green to a colorless transparent solution after 30 minutes. The reaction mixture was stirred for 24 hrs. A colorless precipitate was isolated by vacuum filtration inside the dry-box. The precipitate was washed with pentane and a colorless solid was isolated. Crystals were grown of the isolated product by performing a layering experiment with CH_2Cl_2 and Ether. One product isolated was actually $(Ph_3P)Cu(\mu-Cl)_2Cu(PPh_3)_2$. It is a known compound, whose structure was first determined by Bellon and coworkers in Italy.[4.4] $NaN(SiMe_3)_2$ (1 M, 1 mL, 1 mmol) was

added to the isolated product (0.361 g, 1 mmol) suspension in 40 mL of pentane in the dry-box. The resulting light green suspension turned yellow approximately 30 min after the addition of the amide. The mixture was allowed to stir for 1 day, at which point a yellow precipitate had formed. This was collected by gravity filtration and the pentane filtrate was evaporated. From the pentane layer, a yellow solid was obtained. The ^{31}P NMR spectrum of the isolated product in CD_2Cl_2 showed a slight downfield shift from free PPh$_3$. The ^{1}H NMR was taken in CD_2Cl_2 and the results were inconclusive. This "(Ph$_3$P)Cu-N(SiMe$_3$)$_2$" product shows yellow luminescence in the solid state when the compound is excited at wavelengths below 400 nm at room temperature. Note: This same procedure was attempted for PEt$_3$, dppe and PEtPh$_2$. However, no conclusive results were obtained.

4.2.3 Attempted Preparation of CuN(SiMe$_3$)$_2$(t-butyl isocyanide)

Copper(I) chloride (0.247 g, 2.5 mmol) was suspended in 40 mL of pentane in a dry-box. After 5 min, t-butyl isocyanide (0.28 mL, 2.5 mmol) was added. The solution changed from light lime green to cloudy. Then, NaN(SiMe$_3$)$_2$ (1 M in THF, 2.5 mL, 2.5 mmol), was added to the mixture and allowed to stir for 1 day. The next day, the solution had changed from cloudy to yellow with a gray precipitate. The precipitate was removed by gravity filtration inside the dry-box. The pentane filtrate was evaporated and a yellow solid-like material was isolated. ^{1}H NMR spectrum showed 1:2 ratio of t-butyl group to the trimethylsilyl groups in the spectrum. IR: $\nu_{CN} = 2198$ cm^{-1} vs. free t-BuNC 2130 cm^{-1} (Sadtler IR spectra, No. 76965K). Efforts to duplicate this synthesis were unsuccessful.

4.2.4 Preparation of [Cu(CH₃CN)₄]PF₆

This compound was synthesized according to the literature.[4,5] ^{1}H NMR (CD₃CN): 2.2 (s, CH₃CN protons); ^{31}P NMR (CD₃CN): –75.1 (sept, PF₆, J_{P-F} 1620 Hz).

4.2.5 Attempted Preparation of [Cu(CH₃CN)ₓ(dppe)]ₙ(PF₆)ₙ

This method is based on the literature procedure for [Cu₂(dppm)₂(CH₃CN)₂](PF₆)₂.[4,6] [Cu(CH₃CN)₄]PF₆ (0.232 g, 0.625 mmol) was suspended in 40 mL of CH₂Cl₂ inside the drybox. After 5 minutes, a colorless solution formed and dppe (0.259 g, 0.625 mmol) was added. The colorless transparent solution was stirred for 6 hours and then concentrated to 15-20 mL. Diethyl ether was added to the transparent solution and a colorless precipitate formed, which was isolated by gravity filtration. ^{1}H NMR (CD₂Cl₂): 7.2, 7.4 (d, 20H, Ph), 2.3, 2.4 (d, 4H, -CH₂CH₂-), 2.0 (s, ca. 5H, CH₃CN protons); ^{31}P NMR (CD₂Cl₂): -8.6 (broad s, dppe), –71.1 (sept PF₆, J_{P-F}(1620 Hz)). The ^{1}H NMR integration for the dppe and CH₃CN resonances suggested a stoichiometry between [Cu(CH₃CN)(dppe)]ₙ(PF₆)ₙ and [Cu(CH₃CN)₂(dppe)]ₙ(PF₆)ₙ for the product. Also, IR data was gathered for this complex and a v_{CN}(IR) = 2272 cm^{-1} was observed. This colorless compound exhibits yellow luminescence in the solid state. The analogous reaction was attempted with dmpe. ^{1}H NMR (CD₂Cl₂): 1.73 (s, broad, 4H, CH₃CN), 1.55 (s, 4H, -CH₂CH₂-), 1.32 (m, 12H, CH₃); ^{31}P NMR (CD₂Cl₂): –5.97, –12.4, –21.9, –29.2 (quartet, Cu(dmpe)₂⁺), -71.1 (sept PF₆⁻, J_{P-F}(1620 Hz)). Dmpe was identified in the ^{1}H NMR spectrum; however, the number of CH₃CN ligands was inconclusive.

4.2.6 Attempted Preparation of (dppe)CuN(SiMe₃)₂

[Cu(CH₃CN)ₓ(dppe)]ₙ(PF₆)ₙ (0.146 g, 0.125 mmol) was dissolved in CH₂Cl₂ room temperature. The solution was cooled to –5 °C and NaN(SiMe₃)₂ (1 M in THF;

0.125 mmol, 0.125 mL) was added dropwise during 30 minutes. A green precipitate formed. The precipitate was removed by gravity filtration and the yellow filtrate was evaporated to give a yellow solid. ^{1}H NMR (CD$_2$Cl$_2$): 7.3 (m, 20H, Ph), 2.45 (s, 4H, -CH$_2$CH$_2$-), 0.01 (s, 18H, CH$_3$). The NMR results gave the integration for 1:1 ratio of donor ligand (dppe) to $^-$N(SiMe$_3$)$_2$. However, these results could not be duplicated.

Since there was difficulty in isolating the dppe complex, an effort was made to duplicate the literature synthesized complex, [Cu$_2$(CH$_3$CN)$_2$(dppm)$_2$](PF$_6$)$_2$.[4,6] An ^{1}H NMR was taken of the complex and compared to the literature. The complex was synthesized once, however effects to reproduce this complex were unsuccessful.

We tried to find other avenues to identify the complexes isolated in each experiment. In most of the ^{31}P NMR spectra, there was a slight downfield shift observed for the coordinating phosphine ligand to the Cu center. The phosphine ligands may be exchanging rapidly in solution. Also, in the ^{1}H NMR spectra, the number of acetonitrile ligands in the intermediate complex, [Cu(CH$_3$CN)$_x$(phosphine)]$_n$(PF$_6$) was wrong.

4.3 Results

In order to prepare the desired L$_n$CuN(SiMe$_3$)$_2$ complexes, we explored two synthetic strategies with CuCl as starting material, each of which should give the overall reaction:

$$CuCl + nL + Na^+(SiMe_3)_2N^- \rightarrow LnCuN(SiMe_3)_2 + NaCl \qquad \text{Equation 4.2}$$
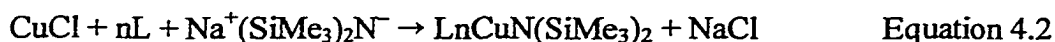
1) Treatment of Cu with L and then NaN(SiMe$_3$)$_2$ in pentane or THF; or 2) Treatment of CuCl with L, isolation of the intermediate product, LCuCl, and subsequent treatment of the intermediate with NaN(SiMe$_3$)$_2$ in pentane or THF.

4.3.1 Results with CuCl

The results of these experiments are summarized in Table 4.1. Products of the $(CuCl + L + NaN(SiMe_3)_2)$ reactions were very difficult to charaterize. In the ^{31}P NMR spectra, it is hard to determine whether or not the phosphines are bound to the metal center. Ordinarily, the ^{31}P resonances for phosphines shift downfield on coordination to a metal center. In most of these experiments, we saw at best a slight $\Delta\delta$. Thus, the ^{31}P NMR spectra do not provide conclusive evidence that these syntheses were successful. However, Cu(I) phosphine complexes are often fluxional in solution[4.7-4.12]: this may explain some of our difficulties with the NMR data.

Luminescence was observed in the product of the dppe reaction: see Figure 4.2. The PPh$_3$ and dppe products exhibit luminescence in the solid state, which is not observed if any of the reactants is omitted. However, we still do not know the structures of the luminescent products.

Table 4.1 Results of Attempted Preparations of $L_nCuN(SiMe_3)_2$ from CuCl

L	Color of Product	Luminescence	Free L δ (^{31}P)	Product δ (^{31}P)
PPh$_3$	yellow	yellow	-6.6	-10.1
PEt$_3$	bright yellow	yellow	-19.5	none
dppe	light yellow	yellow	-14.5	10.7
PEtPh$_2$	mustard yellow	none	-12.0	-7.8
CN-t-Bu	deep yellow	orange	N/A	$\nu_{CN} = 2198\ cm^{-1}$

4.3.2 Results with [Cu(CH$_3$CN)$_4$]PF$_6$

One possible reason for our difficulties with CuCl as starting material is that the Cl$^-$ may not readily dissociate from Cu in organic solvents. Therefore, using a ligand that
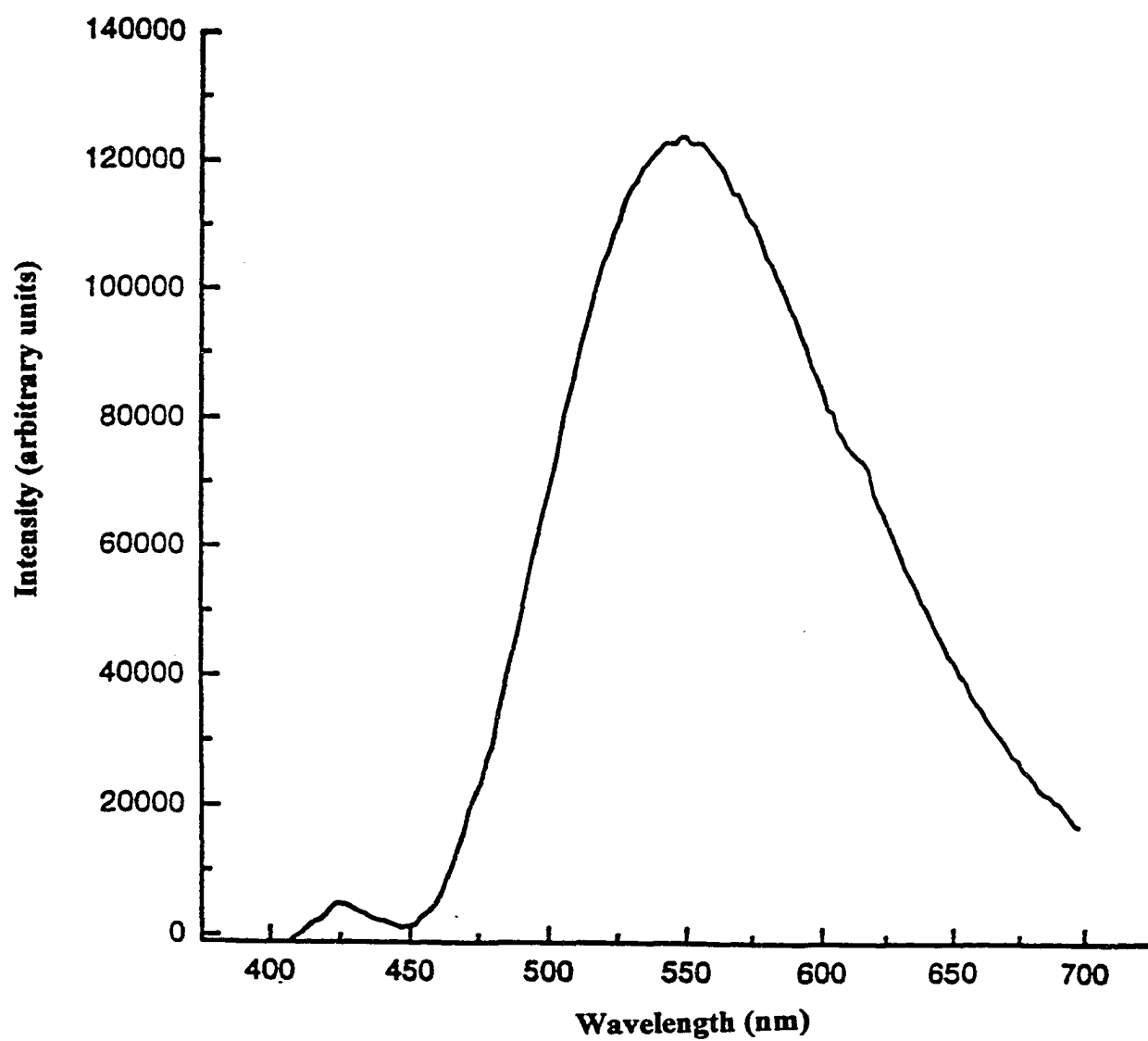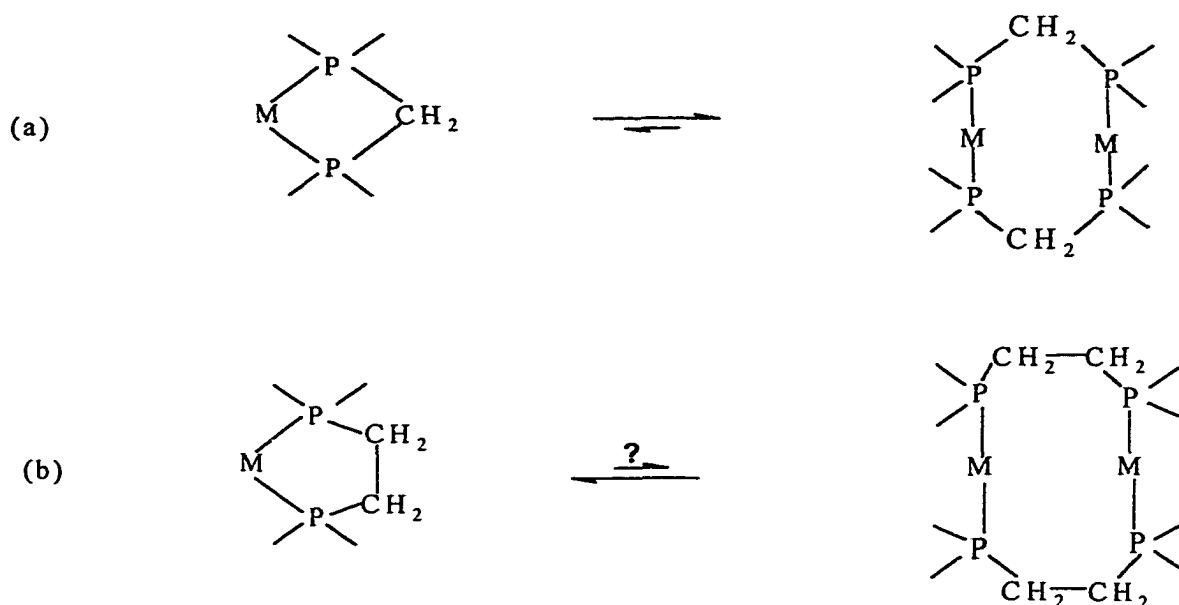
Figure 4.2 Solid state emission spectrum of the dppe–Cu–N(SiMe₃)₂ product.

would easily dissociate from Cu metal center might give better results. Kubas[4.13] in 1970 made tetrakis(acetonitrile)copper(I)hexafluorophosphate, $[Cu(CH_3CN)_4]PF_6$, which readily loses acetonitrile ligands in solution. Díez and coworkers[4.14] used $[Cu(CH_3CN)_4]PF_6$ to make a copper(I) complex of bis(diphenylphosphino)methane (dppm): $[Cu_2(CH_3CN)_2(dppm)_2](PF_6)_2$. We have studied the analogous compounds with dppe and dmpe. Our selection of dppe and dmpe as ligands is based on a consideration of the equilibria in Scheme 4.3. When dppm is the ligand, as in the Díez system, a dimeric structure is favored (See Scheme 4.3a), because the monomeric form would require a strained 4-membered ring. With dppe, on the other hand (See Scheme 4.3b), the monomeric structure has a less strained 5-membered ring. Thus, our new $[Cu(dppe)(CH_3CN)_x]_n(PF_6)_n$ and $[Cu(dmpe)(CH_3CN)_x]_n(PF_6)_n$ complexes are more likely to be monomers (i.e. n=1). The results are summarized in Table 4.5.

4.3.2.1 $[Cu(CH_3CN)_4](PF_6)$ with dppe

The ^1H NMR of $[Cu(dppe)(CH_3CN)_x]_n(PF_6)_n$ does not indicate whether the complex is a monomer or dimer. The CH_3CN and $CH_2(dppe)$ resonances integrate in the ratio 5:4. This may mean that a mixture of $[Cu(CH_3CN)_2(dppe)]_n(PF_6)_n$ (expected ratio of 6:4) and $[Cu(CH_3CN)(dppe)]_n(PF_6)_n$ (expected a ratio of 3:4) is present. One of the compounds isolated in the mixture was $[Cu_2(CH_3CN)_4(dppe)](PF_6)_2$. Even though this complex was not the desired compound, it is of lower nuclearity. An ORTEP projection of the molecule is shown in Figure 4.3; Table 4.2-4.4 lists the crystallographic data, selected bond distances, and atom coordinates. Our $[Cu_2(CH_3CN)_4(dppe)]_n(PF_6)_n$ product exhibits yellow luminescence in the solid state when it is excited below 400 nm at room temperature.

(a)

(b)

Scheme 4.3

Attempts were made to determine the stoichiometry of the luminescent product; however, they were unsuccessful. The solid state emission spectrum was obtained of the complex mixture (Figure 4.4).

4.3.2.2 [Cu(CH$_3$CN)$_4$]PF$_6$ with dmpe

^{1}H and ^{31}P NMR were taken of [Cu(CH$_3$CN)$_4$](PF$_6$)–dmpe reaction product. The ^{31}P NMR spectrum of the product showed a quartet due to coupling of the ^{31}P of the dmpe phosphorus to ^{63,65}Cu(I = 3/2) and a septet for PF$_6^-$ phosphorus (Table 4.2). Since $J(^{31}$P-^{63,65}Cu) was observed, the complex isolated was likely to be a highly symmetrical one, such as [Cu(dmpe)$_2$](PF$_6$).

4.3.2.3 [Cu(CH$_3$CN)$_x$(dppe)]$_n$(PF$_6$)$_n$ + NaN(SiMe$_3$)$_2$

Initial results from the reaction of ([Cu(CH$_3$CN)$_x$(dppe)]$_n$[PF$_6$]$_n$ + NaN(SiMe$_3$)$_2$), as judged by ^{1}H NMR, are that the CH$_3$CN ligand dissociated in the reaction mixture
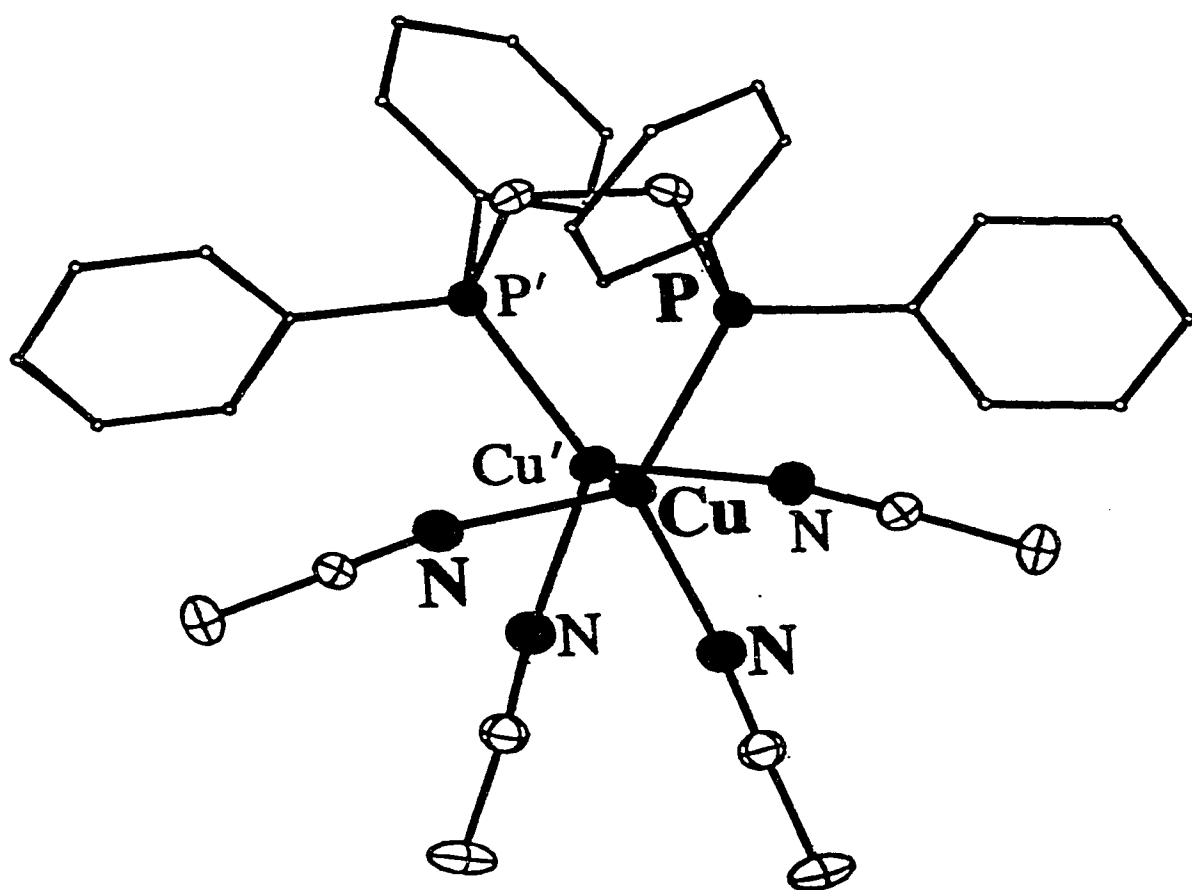
Figure 4.3 ORTEP drawing of $[Cu_2(CH_3CN)_4(dppe)]^{2+}$
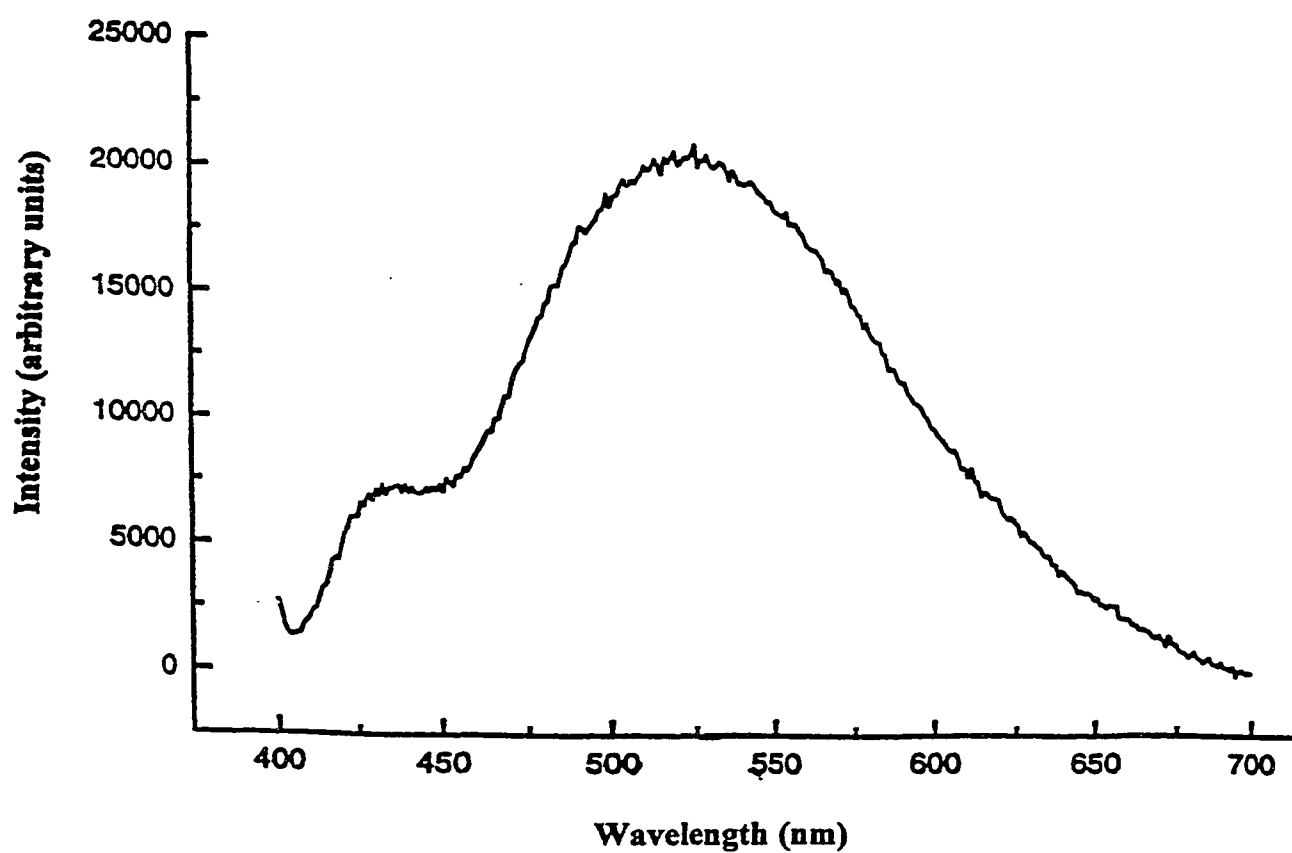
Figure 4.4 Solid state emission spectrum of $[Cu_2(CH_3CN)_4(dppe)](PF_6)_2$

Table 4.2 Crystal Data for $[Cu_2(CH_3CN)_4(dppe)](PF_6)_2$[a]

formula	$Cu_2C_{34}N_4P_4F_{12}H_{36}$
fw	979.65
space group	Fdd2
Z	8
T/K	298
$\lambda/\text{Å}$	1.54184 (Cu Kα)
a/Å	26.022(2)
b/Å	28.436(2)
c/Å	11.5414(7)
V/Å	8540(1)
$\rho_x/\text{g cm}^{-3}$	1.524
μ/cm^{-1}	3.406
transm coeff	0.7308-1.0000
R(F) (obs data)[b]	0.065
Rw(F)[c]	0.084

[a]In Tables 4.2-4.4 estimated standard deviations in the least significant digits of the values are given in parentheses. [b]$R = \Sigma||F_o|-|F_c||/\Sigma|F_o|$; data with I>1$\sigma$(I). [c]$R = \sqrt{(\Sigma_w(|F_o|-|F_c|)^2/\Sigma_w F_o^2)}$; w = $4F_o^2/\sigma^2(I) + (0.02F_o^2))^2$

Table 4.3 Atomic Coordinates for $[Cu_2(CH_3CN)_4(dppe)](PF_6)_2$

	x	y	z	Ueq
Cu	0.24637(3)	0.19961(3)	0.0000	0.0601(4)
P1	0.28924(5)	0.19462(4)	0.1639(1)	0.0471(5)
P2	0.36990(9)	0.30916(8)	0.5299(2)	0.104(1)
N1	0.2737(2)	0.1915(2)	-0.1567(4)	0.076(3)
N2	0.1716(2)	0.2090(2)	-0.0287(4)	0.078(3)
C1	0.2785(2)	0.2424(2)	0.2675(4)	0.054(2)
C2	0.2695(2)	0.2675(4)	0.2455(5)	0.058(3)
C3	0.2243(2)	0.1205(2)	0.2184(6)	0.072(4)
C4	0.2057(3)	0.0820(3)	0.2800(8)	0.092(5)
C5	0.2352(4)	0.0660(3)	0.3696(8)	0.109(5)
C6	0.2825(4)	0.0865(3)	0.4001(6)	0.094(5)
C7	0.2999(3)	0.1266(2)	0.3377(6)	0.075(4)
C8	0.3582(2)	0.1892(2)	0.1542(5)	0.054(2)
C9	0.3922(2)	0.2113(2)	0.2270(6)	0.072(3)
C10	0.4423(3)	0.2038(2)	0.2190(9)	0.092(5)
C11	0.4617(3)	0.1750(3)	0.1293(9)	0.113(5)
C12	0.4276(3)	0.1533(3)	0.0597(9)	0.102(5)
C13	0.3776(2)	0.1616(2)	0.0659(6)	0.071(3)
C14	0.4644(3)	0.4356(2)	0.4997(6)	0.074(3)
C15	0.3038(4)	0.1761(3)	-0.3666(6)	0.105(6)
C16	0.3823(2)	0.0336(2)	0.1882(5)	0.067(3)
C17	0.3320(3)	0.0222(3)	0.1461(8)	0.090(4)

Table 4.4 Selected Interatomic Distances/Å for $[Cu_2(CH_3CN)_4(dppe)](PF_6)_2$

Cu-Cu′	2.872(1)
Cu-P1	2.200(1)
Cu-N1	1.957(5)
Cu-N2	1.992(5)
P1-C1	1.832(5)
P1-C2	1.808(5)
P1-C8	1.804(5)
N1-C14	1.135(9)
N2-C16	1.110(8)
C1-C1′	1.543(8)

Table 4.5 Results of Attempted Preparations of LCuN(SiMe$_3$)$_2$ from
[Cu(CH$_3$CN)$_4$]PF$_6$ as Starting Material

L	Color of Product	Luminescence	Free L δ(^{31}P)	Product δ(^{31}P)
[Cu(CH$_3$CN)$_x$(dppe)]$_n$(PF$_6$)$_n$	colorless	yellow	-14.5	-8.6
[Cu(CH$_3$CN)$_x$(dppm)]$_n$(PF$_6$)$_n$	colorless	yellow	-23.5	-11.2
[Cu(CH$_3$CN)$_x$(dmpe)]$_n$(PF$_6$)$_n$	colorless	yellow	-49.1	Quartet, -5.97, -12.4, -21.9, -29.2

because CH$_3$CN was no longer observed in the NMR spectrum. Also, the integration

between the methyl groups on the silyl amide and the phenyl group on the dppe ligand

was correct. Although the initial experiment was promising, efforts to repeat the results

that were obtained were unsuccessful.

4.3.2.4 [Cu(CH$_3$CN)$_x$(dmpe)]$_n$(PF$_6$)$_n$ + NaN(SiMe$_3$)$_2$

Initially, blue-green luminescence was observed in the reaction mixture which is

indicative of trace amounts of [CuN(SiMe$_3$)$_2$]$_4$. This was removed by extraction with

CH$_2$Cl$_2$. The precipitate isolated from the extraction exhibited yellow luminescence.

^{1}H and ^{31}P NMR were taken of the reaction mixture. In the ^{1}H NMR spectrum gave

inconclusive results. However, in the ^{31}P NMR the coupling between the Cu and the

phosphorus on the dmpe was no longer observed. This shows that the symmetrical

complex was no longer observed.

4.4 Discussion

Several research groups have isolated lower nuclearity Cu(I) complexes. Lopes et

al. isolated [Cu(OC$_6$H$_3$Ph$_2$)(CO)]$_2$ from [(CuOC$_6$H$_3$Ph$_2$)]$_4$ by a carbonylation reaction.[4.13]

Yamamoto et al. isolated several monomeric Cu(I) complexes. The complex that was the

most stable was $[Cu(PPh_3)_2(N(C_6H_5)(H))]$.[4.10] In most cases, the complex contains some

type of electron-withdrawing group or the complexes exist as salts.[4.14]

Due to the autocomplexation of metal amides, there is difficulty in isolating lower

nuclearity Cu-amide complexes. When attempts were made to add $NaN(SiMe_3)_2$ to the

salt complex, mixtures were isolated (which was observed in the NMR integration). All

products isolated exhibited luminescence in the solid state; however, their stoichiometry

was unable to be determined.

4.5 Conclusions

We have explored making lower nuclearity derivatives of $[CuN(SiMe_3)_2]_4$. We

were able to isolate $[Cu_2(CH_3CN)_4(dppe)](PF_6)_2$ as one product in the reaction mixture.

However, we failed to isolate $L_nCuN(SiMe_3)_2$. Thus, isolating useful Cu CVD precursors

from these reactants is likely to be difficult.

4.6 References

[4.1] Jeffries, P. M.; Girolami, G. S. *Chem. Mater.,* **1989**, 1, 8-10.

[4.2] Beach, D. B.; LeGoues, F. K.; Hu, C. –K., *Chem. Mater.,* **1990**, 3, 216-219.

[4.3] Lappert, M. F.; Power, P. P.; Sanger, A. R.; Srivastava, R. C. *Metals and Metalloid Amides: Synthesis, Structures, and Physical and Chemical Properties,* Ellis Horwood Series in Chemical Science, New York, **1980**.

[4.4] Albano, V. G.; Bellon, P. L.; Ciani, G.; Manassero, M. *J. Chem. Soc. Dalton Trans.,* **1972**, 171-175.

[4.5] Kubas, G. J. *Inorg. Synth.,* **1979**, 19, 90.

[4.6] Díez, E.; Gamasa, M. P.; Gimeno, J. *J. Chem. Soc. Dalton Trans.,* **1987**, 1275-1278.

[4.7] Garrou, P. E. *Chem. Rev.,* **1981**, 81, 229-266.

[4.8] Shaw, G. *Chem. Comm.,* **1966**, 425-426.

[4.9] Batchelor, R.; Birchall, T. *J. Am. Chem. Soc.,* **1982**, 104, 674-679.

[4.10] Yamamoto, T.; Ehara, Y.; Kubota, M.; Yamamoto, A. *Bull. Chem. Soc. Jpn.*, **1980**, 53, 1299-1302.

[4.11] Costa, G.; Reisenhofer, E.; Stefan, L. *J. Inorg. Nucl. Chem.*, **1965**, 27, 2581-2184.

[4.12] Costa, G.; Pellizer, G.; Rubessa, F. *J. Inorg. Nucl. Chem.*, **1964**, 26, 961-964.

[4.13] Lopes, C.; Håkansson, M.; Jagner, S. *Inorg. Chem.*, **1997**, 36, 3232-3236.

[4.14] Hope, H.; Olmstead, M. M.; Power, P. P.; Sandel, J.; Xu, X. *J. Am. Chem. Soc.*, **1985**, 107, 4337-4338.

[4.15] James, A. M., Laxman, R., Fronczek, F. R., Maverick, A. W. *Inorg. Chem.*, **1998**, 37, 3785-3791.

Chapter 5

Cu(hfac)₂ Adducts with Diols and Ether-Alchols and Their Use in Copper CVD

5.1 Introduction

The precursors for Cu CVD that have been studied so far are mostly metal organic complexes. There are two classes of metal organic complexes based on the 1,1,1,5,5,5 hexafluoro-2,4-pentadionate ($hfac^-$) ligand: 1.) Cu(II) complexes i.e. $Cu(hfac)_2$ and its adducts with water and other donor molecules and 2.) Cu(I) complexes i.e. Cu(hfac)L (L = alkene, alkyne, phosphine). It has been reported that deposition rate and purity of Cu metal increased with the use of protic co-reactants such as water and alcohols from Cu(II) and Cu(I) precursors.[5.1] This chapter explores the use of diols and ether-alcohols in possible self-reducing precursors that could enhance the deposition of Cu metal without the use of a reducing gas.

Alcohol-assisted CVD using $Cu(hfac)_2$ precursors has been conducted previously to probe the role of alcohols as reducing agents. In earlier work, Cho reported the use of i-PrOH as an additive with $Cu(hfac)_2$ and H_2 that led to of Cu CVD metal at 225 °C on SiO_2.[5.2] However, it was unclear whether or not i-PrOH was used stoichiometrically as a reactant or a catalyst.

Fan reported $Cu(hfac)_2$-i-PrOH as the first liquid copper(II) precursor.[5.3] Deposition occurs by passing a stream of carrier gas over the precursor, followed by reaction over a heated substrate. There are some unique characteristics about this precursor. It shows a higher deposition rate under N_2 carrier gas than with H_2. The minimum temperature required for deposition is 160 °C under N_2 compared to 200 °C

71

under H_2. The precursor was identified as being self-reducing by the production of

acetone (from oxidation of i-PrOH) when N_2 was used as the carrier gas.

The importance of the i-PrOH is the α hydrogen in close proximity to the copper

metal center. In this case, the α hydrogen, as well as the hydroxide hydrogen, is liberated

reducing the Cu(II) to Cu metal and oxidizing i-PrOH to acetone (Equation 5.1).

$$Cu(hfac)_2 \cdot i\text{-PrOH} \rightarrow Cu + 2hfacH + CH_3COCH_3 \qquad \text{(Equation 5.1)}$$
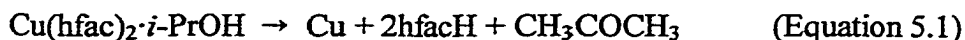
Fan was able to identify acetone in the reaction products. However, he had to use excess

i-PrOH to obtain pure Cu films at high deposition rates because i-PrOH dissociates

readily from the Cu complex well below the typical evaporation temperature for Cu

CVD. We reasoned that, if a more stable adduct of Cu(hfac)$_2$ can be used, then excess

alcohol may not be necessary for CVD.

My research has focused on the use of ether-alcohols and diols to produce

potential self-reducing adducts for Cu CVD. Even though ether-alcohols are more

volatile than diols, the presence of two oxygen donor ligands should give greater adduct

stability and aid in the deposition to Cu metal. Ethylene glycol (1), 2-methoxyethanol

(2), propylene glycol (3), and 1-methoxy-2-propanol (4) (Figure 5.1) were used as Lewis
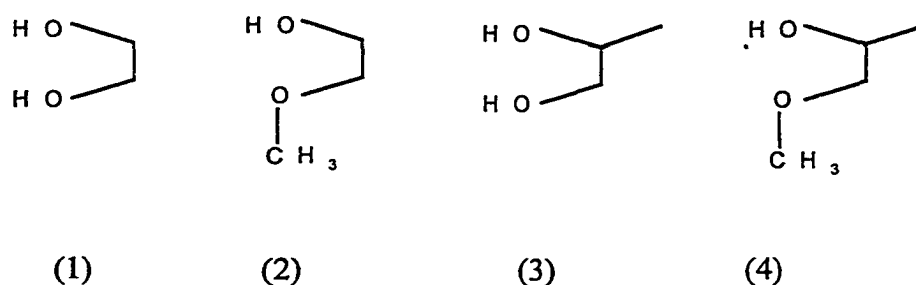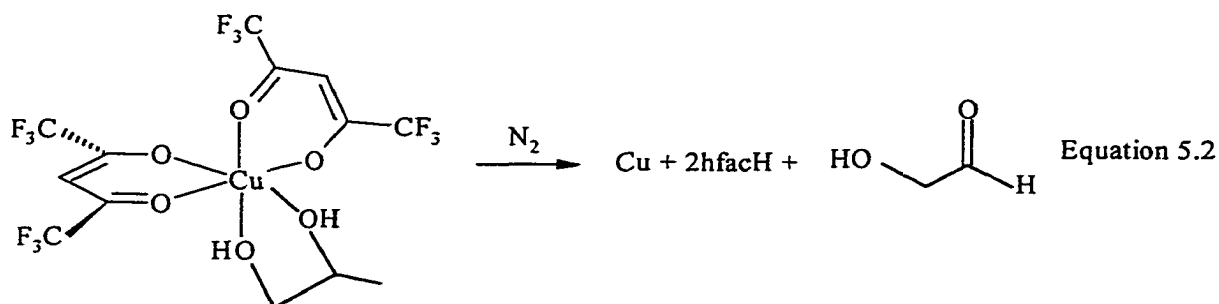
bases, forming

Figure 5.1 Ether-Alcohols and Diols

adducts with $Cu(hfac)_2$. These molecules were chosen because they have the potential of being bidentate ligands. Especially if both oxygen atoms coordinate to the Cu metal center, the adducts may be more stable to dissociation than $Cu(hfac)_2 \cdot i\text{-PrOH}$. These

Equation 5.2

adducts were also expected to have self-reducing properties similar to those with simple alcohols. For example, if $Cu(hfac)_2 \cdot$propylene glycol was a bidentate ligand and the complex was self reducing, it would reduce $Cu(II)$ to $Cu(0)$ and oxidize propylene glycol to hydroxyacetone (Equation 5.2). Thermal CVD experiments were carried out using these adducts as precursors. The thickness and resistivities of the resulting films were measured. Hydrogen gas was necessary for the formation of pure Cu films. The $Cu(hfac)_2 \cdot$propylene glycol adduct demonstrated better deposition ability than the other adducts.

5.2 Experimental

5.2.1 General Procedure

All reactions were carried out using standard dry-box techniques. Anhydrous solvents were obtained from Aldrich Chemical Company. The other solvents were reagent or HPLC grade and were used without further purification. $Cu(hfac)_2 \cdot H_2O$ was purchased from Strem Chemicals or prepared in the laboratory according to the

literature.[5,4] Cu(hfac)$_2$·H$_2$O was dehydrated in a vacuum desiccator over concentrated sulfuric acid or phosphorus pentoxide overnight.

The Cu(hfac)$_2$·ROH adducts were prepared by dissolving anhydrous Cu(hfac)$_2$ in CH$_2$Cl$_2$ inside a dry-box. Stoichiometric quantities of each ether alcohol or diol were added to the dark blue solution. The solutions were stirred overnight and the excess solvent was removed by vacuum forming various shades of green solids. The physical data of each Cu(hfac)$_2$ adduct is shown in Table 5.1. Each solid was purified by vacuum sublimation. Minimizing exposure to air is very important because alcohols are readily displaced from the adducts by H$_2$O. However, when the compounds were kept under inert atmosphere as much as possible, no loss of adduct ligand occurred as confirmed by the reproducibility of the melting points shown in Table 5.1. All of the adducts were characterized by microanalysis as shown Table 5.2. The analysis shows that there is one molecule of the oxygen donor for every molecule of Cu(hfac)$_2$.

5.2.2 X-Ray Analysis

Crystals of Cu(hfac)$_2$·2-methoxyethanol suitable for X-ray analysis were grown by slow evaporation of a dichloromethane solution. Diffraction data (see summary in Table 5.3) were collected on an Enraf-Nonius CAD4 diffractometer fitted with Mo Kα source and graphite monochromator, using the θ-2θ scan method. The crystal was cooled in a thermostatted N$_2$ cold stream. Final unit cell constants were determined from the orientations of twenty-five centered high-angle reflections. The intensities were corrected for absorption using ψ scan data for five reflections. The SHELXTL set of programs was used for structure and refinement.

Table 5.1 Physical Data of Cu(hfac)$_2$ and Its Adducts

Adducts	Color	Melting Point (°C)	Percent Yield (%)	Sublimation Temperature (°C)
Cu(hfac)$_2$	dark blue	95-98	—	—
Cu(hfac)$_2$·H$_2$O	turquoise green	130-134	—	—
Cu(hfac)$_2$·ethylene glycol	lime green	109-110	80-85	65-70
Cu(hfac)$_2$·2-methoxyethanol	teal green	53-55	70-75	32-35
Cu(hfac)$_2$·propylene glycol	dark green	54-56	65-70	30-35
Cu(hfac)$_2$·1-methoxy-2-propanol	emerald green	35-37	65-70	35-37

Table 5.2 Elemental Analysis of Cu(hfac)$_2$ Adducts

Compound	Calculated %C	%H	Found %C	%H
Cu(hfac)$_2$·ethylene glycol	26.67	1.48	27.10	1.69
Cu(hfac)$_2$·2-methoxyethanol	28.17	1.81	28.02	1.74
Cu(hfac)$_2$·propylene glycol	28.17	1.81	27.96	1.62
Cu(hfac)$_2$·1-methoxy-2-propanol	29.58	2.11	28.92	1.89

5.2.3 CVD Reactions

The CVD reactions were carried out in a vertical cold wall reactor. (Figure 5.2) The precursors were placed in the evaporator that was immersed in a sand bath at 80 °C. The H$_2$ carrier/reducing gas at 400 mL/min (1 atm) was passed through the evaporator, and the vapors were then transported to the reactor. The substrate was attached to an electrically heated metal susceptor in the CVD reactor using silver paint purchased from

SPI Supplies. The temperature of the substrate (200 °C) was monitored by a thermocouple. The delivery line between the evaporator and the reactor was wrapped with heating tape to prevent condensation of the precursor. Each CVD reaction was carried out for 1 hour on borosilicate glass (12 mm). After deposition, the substrates were cooled under H_2 for 30 minutes to inhibit corrosion of the films.

5.2.4 Film Characterization

The thicknesses of the films were measured using a stylus profilometer. On each sample, the thickness was measured at the center and in one position on each side. The average of the five measurements was used to represent the thickness of the film.

The resistivities of the films were measured using a four-point probe. They were done at the same position on each sample where the thicknesses were measured. The resistance (R) read from the instrument was converted to a bulk resistivity value (ρ_{raw}) by multiplying by the corresponding thickness (T) and a correction factor (C.F.) (Equation 5.3).

$$\rho_{raw} = C.F. \times T \times R \qquad \text{(Equation 5.3)}$$

The resistivity values calculated for CVD Cu films from the four-point probe data were often less than the experimental bulk resistivity of pure copper (1.67 $\mu\Omega\cdot cm$). A reference sample of high-purity copper foil also gave anomalously low resistivity. The abnormal results are believed to be caused by a systematic error in the four-point probe. Therefore, the raw resistivity values of the sample (ρ_{raw}) were subsequently corrected by that ($\rho_{Cu} = 1.16$ $\mu\Omega\cdot cm$) of the pure copper foil (12.5 μm thick, 99.9% pure) obtained from the same instrument, using Equation 5.4.

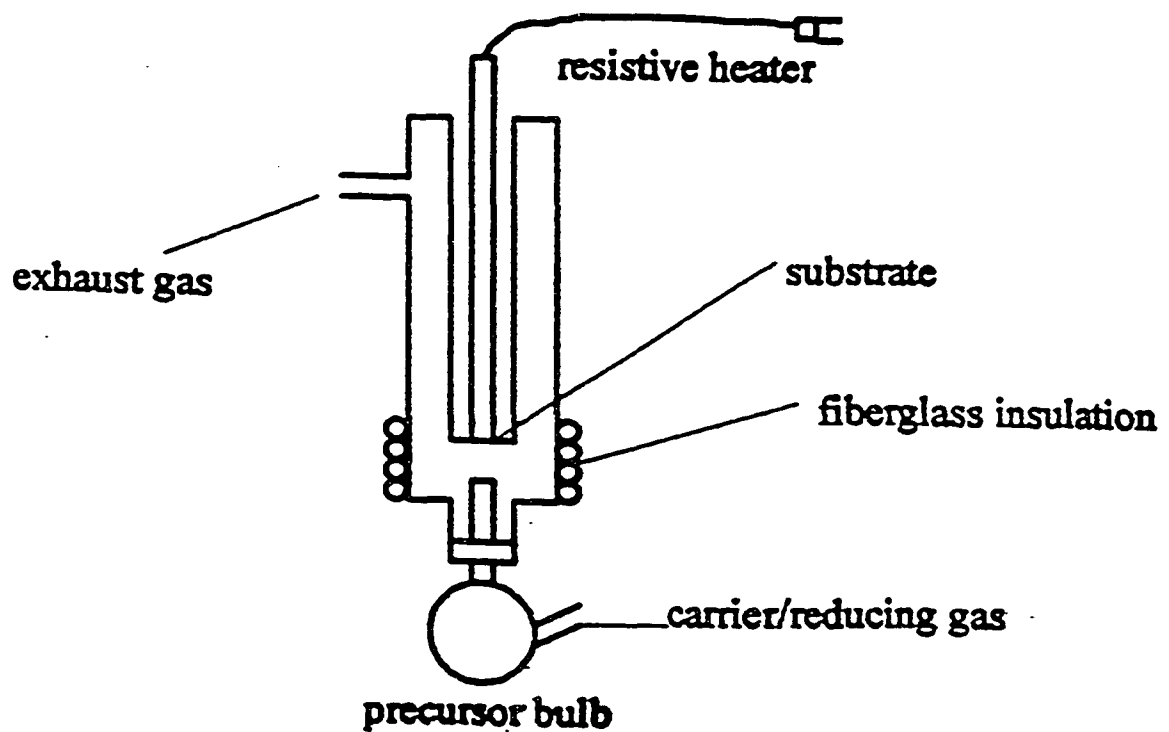$$\rho_{corr} = (1.67 \ \mu\Omega\cdot cm \times \rho_{raw})/\rho_{Cu} \qquad \text{(Equation 5.4)}$$

Figure 5.2 Chemical Vapor Deposition Cold-Wall Reactor

5.3 Results and Discussion

5.3.1 Synthesis and Characterization

Cu(hfac)$_2$ was prepared by placing Cu(hfac)$_2$·H$_2$O in a vacuum desiccator over P$_2$O$_5$ or H$_2$SO$_4$ to give dark blue crystals. Preparation of each adduct was carried out in a drybox by dissolving Cu(hfac)$_2$ in anhydrous CH$_2$Cl$_2$ and adding the appropriate ether alcohol or diol. Each reaction was done at a 1:1 ratio of Cu(hfac)$_2$ to the corresponding ether-alcohol or diol.

5.3.2 Molecular Structures

A number of structural possibilities for such adducts exist, based on previous reports of crystal structures of other five-coordinate adducts of copper(II) β-diketonates. Cu(hfac)$_2$ itself is a square planar complex with the central copper atom coordinated to the four oxygen atoms of the hexafluoroacetylacetonate ligands. Distortion of the ligand field around the copper upon approach of a donor molecule can occur such that: (1) the donor becomes the axial ligand in a square pyramidal complex;[5.5, 5.6] (2) the donor becomes an equatorial ligand in a square pyramidal complex and one of the oxygens from the chelate ligands becomes the axial ligand;[5.7, 5.8] (3) addition of a donor molecule forms a trigonal bipyramidal structure.[5.9] All structurally characterized five-coordinate adducts Cu(biketonate)$_2$L in which L is an O-donor (H$_2$O, alcohols, ethers) are of the first type, square pyramidal with apical L. See structural data in Table 5.6.

The adducts studied here contain donor molecules that could be bidentate. Thus in the present study, an additional structure is possible. The crystal structure of the Cu(hfac)$_2$·2-methoxyethanol was determined. An ORTEP projection of the molecule shown in Figure 5.3; Tables 5.3-5.5 list the crystallographic data, bond distances, and
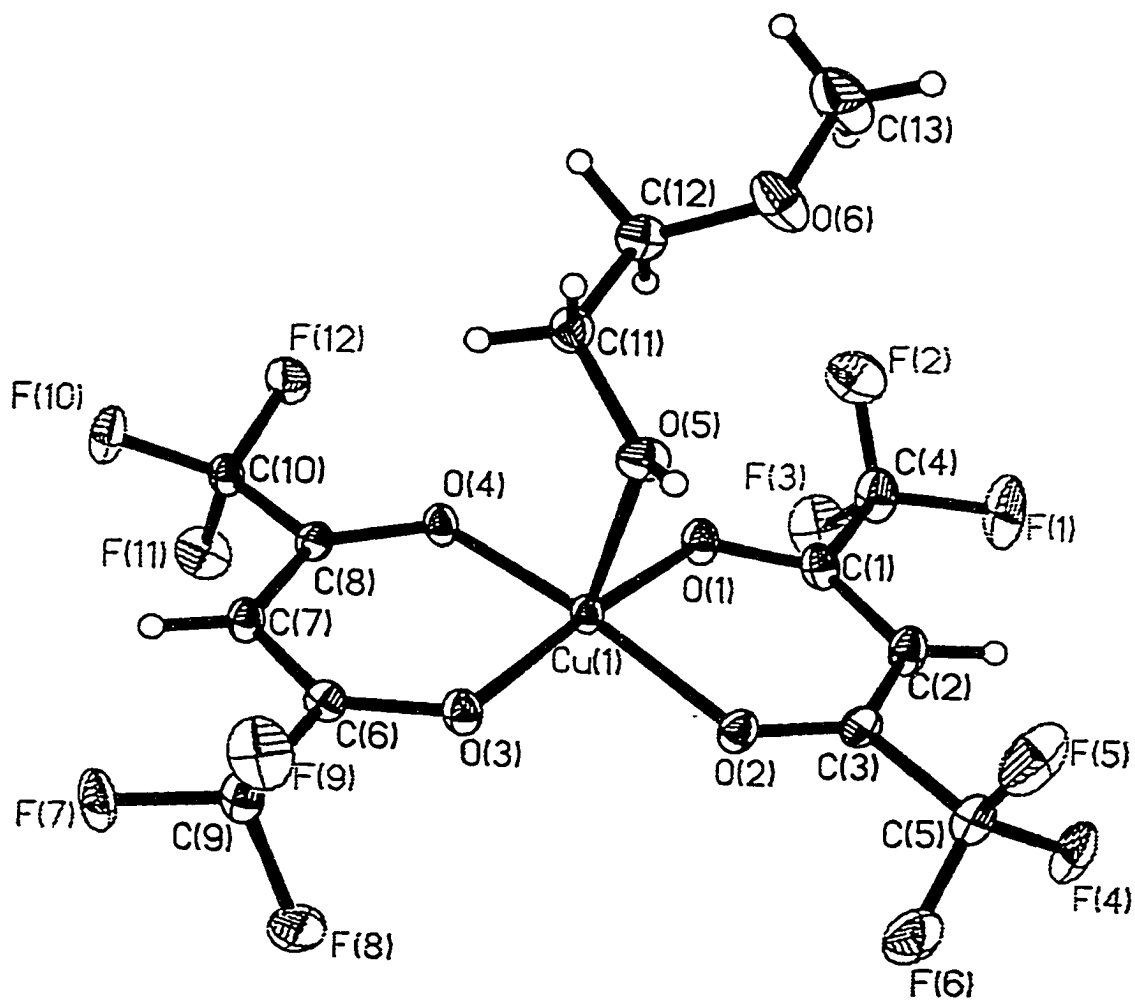
Figure 5.3 ORTEP drawing of Cu(hfac)₂·2-methoxyethanol

Table 5.3 Crystal Data for Cu(hfac)$_2$·2-methoxyethanol[a]

formula	CuC$_{13}$F$_{12}$H$_{10}$O$_6$
fw	553.76
space group	P2$_1$/n
Z	4
T/K	100
λ/Å	0.71073 (Mo Kα)
a/Å	9.295(6)
b/Å	23.998(2)
c/Å	9.351(6)
β/°	114.763(6)
V/Å^3	1894(2)
ρ_x/g cm^{-3}	1.942
μ/cm^{-1}	1.299
transm coeff	0.733-0.894
R(F) (obs data)[b]	0.0327
R$_w$(F)[c]	0.0874

[a]In Tables 5.3-5.5, estimated standard deviations in the least significant digits of the values are given in parentheses. [b]$R = \Sigma ||F_o| - |F_c|| / \Sigma |F_o|$; data with I>2$\sigma$(I). [c]$R_w = \sqrt{(\Sigma_w(|F_o| - |F_c|)^2 / \Sigma wF_o^2)}$; $w = 4F_o^2/(\sigma^2(I) + (0.02F_o^2))^2$

Table 5.4 Atomic Coordinates for $Cu(hfac)_2 \cdot 2$-methoxyethanol

	x	y	z	U_{eq}
Cu1	0.56258(2)	0.146190(9)	0.90544(2)	0.01403(7)
O1	0.63448(15)	0.11664(5)	0.75280(15)	0.0183(2)
O2	0.34075(14)	0.13599(5)	0.76490(14)	0.0177(2)
O3	0.48865(14)	0.18598(5)	1.04301(14)	0.0170(2)
O4	0.77976(14)	0.16827(5)	1.02832(14)	0.0167(2)
O5	0.5696(2)	0.06435(6)	1.0135(2)	0.0205(3)
O6	0.7142(2)	-0.04009(6)	0.9930(2)	0.0306(3)
C1	0.5448(2)	0.09715(7)	0.6211(2)	0.0182(3)
C2	0.3798(2)	0.09340(8)	0.5531(2)	0.0204(3)
C3	0.2923(2)	0.11280(7)	0.6321(2)	0.0158(3)
C4	0.6346(2)	0.07477(9)	0.5280(2)	0.0259(4)
C5	0.1118(2)	0.10357(8)	0.5543(2)	0.0205(3)
C6	0.5752(2)	0.21403(7)	1.1621(2)	0.0144(3)
C7	0.7379(2)	0.22298(7)	1.2214(2)	0.0157(3)
C8	0.8259(2)	0.20017(7)	1.1464(2)	0.0135(3)
C9	0.4822(2)	0.23994(8)	1.2479(2)	0.0190(3)
C10	1.0011(2)	0.21699(7)	1.2070(2)	0.0160(3)
C11	0.7082(2)	0.04096(8)	1.1355(2)	0.0203(3)
C12	0.8007(2)	0.00877(8)	1.0645(2)	0.0202(3)
C13	0.8014(3)	-0.07877(11)	0.9455(4)	0.0386(6)

Table 5.5 Interatomic Distances/Å for $Cu(hfac)_2 \cdot 2$-methoxyethanol

Cu1-O4	1.9321(12)
Cu1-O2	1.9412(12)
Cu1-O3	1.9440(12)
Cu1-O1	1.9458(12)
Cu1-O5	2.1974(14)
O1-C1	1.253(2)
O2-C3	1.259(2)
O3-C6	1.261(2)
O4-C8	1.262(2)
O5-C11	1.430(2)
O6-C13	1.420(2)
O6-C12	1.421(2)
C1-C2	1.395(2)
C1-C4	1.534(2)
C2-C3	1.389(2)
C3-C5	1.539(2)
C6-C7	1.392(2)
C6-C9	1.535(2)
C7-C8	1.394(2)
C8-C10	1.537(2)
C11-C12	1.502(3)

atom coordinates. The molecule is a distorted square pyramid around the copper, with the four oxygen atoms of the hexafluoroacetylacetonate ligands forming an equatorial plane capped by the alcohol oxygen of the axial 2-methoxyethanol ligand. This is the geometry previously observed for $Cu(hfac)_2$·ethanol[5.10] and $Cu(acac)_2(quinoline)$[5.11]. The axial Cu-O bond to 2-methoxyethanol (2.1971 Å) is elongated compared to the average Cu-O bond length for the hfac ligands (1.94 Å). Such tetragonal distortion has been reported previously for both five- and six-coordinate complexes. In general, five-coordinate complexes exhibit shorter Cu-L bond lengths. Comparison with other reported five-coordinate complexes shows that $Cu(hfac)_2$·2-methoxyethanol has a very short Cu-L bond for a complex in which the adduct is the axial ligand. Table 5.6 list the bond lengths of other axial five-coordinate $Cu(hfac)_2$ adducts. In the $Cu(acac)_2$·(quinoline) and $(Cu(hfac)_2)_2$·pyrazine the Cu-adduct bond length are longer than the $Cu(hfac)_2$·2-methoxyethanol; 2.25(2) Å and 2.36 Å respectively. The Cu-apical O bond distance in $Cu(hfac)_2$·ethanol (2.191 Å) is similar to that in $Cu(hfac)_2$·2-methoxyethanol. It is noteworthy that, though alcohols are generally weakly coordinating compared to amines, the copper-adduct bond length is significantly shorter in $Cu(hfac)_2$·2-methoxyethanol than in either of the other two examples of axially coordinated N-adducts. The small size of the 2-methoxyethanol compared to quinoline and pyrazine may be responsible for this relatively short bond.

5.3.3 Chemical Vapor Deposition with Adducts

CVD experiments were tried with each alcohol adduct to test their effectiveness as precursors. Copper metal films were obtained for the adducts. Table 5.7 shows the average film thickness and resistivity of 3 films obtained from each precursor. All

Table 5.6 Apical Bond Lengths of Five-Coordinate $Cu(diketonate)_2 \cdot L$

$Cu(diketonate)_2 \cdot L$	Bond Length (Å)
$Cu(hfac)_2 \cdot 2$-methoxyethanol	2.1974
$Cu(hfac)_2 \cdot ethanol^{5.10}$	2.191
$Cu(hfac)_2 \cdot n\text{-}BuOH^{5.13}$	2.200(1)
$Cu(hfac)_2 \cdot H_2O^{5.14}$	2.221(6)
$(Cu(hfac)_2)_2 \cdot pyrazine^{5.5}$	2.25(2)
$Cu(acac)_2 \cdot quinoline^{5.11}$	2.36
$[Cu(TDFND)_2 \cdot EtOH]^{5.15}$	2.212(6)

experiments were done at a substrate temperature of 200 °C, evaporation temperature of

80 °C and used H_2 as the carrier and reducing gas at a flow rate of 400 mL min^{-1}. The

precursors were heated in an oil or sand bath. Under the same conditions, no films could

be obtained under N_2 gas. The evaporation temperature was as high as 130 °C and

substrate temperatures as high as 235 °C and no Cu films were obtained under N_2 gas.

We originally chose the ether alcohols and diols because we thought they would

be bidentate ligands (since there are two oxygen donor sites on each ligand). They would

be able to stabilize the $Cu(hfac)_2$, so that excess adduct molecule might not be required in

the CVD process. However, these complexes are monodentate, e.g. only

one alcoholic oxygen is coordinated to the Cu metal center of $Cu(hfac)_2$ (Figure 5.3).

Even though the precursors are monodentate, they are more stable than $Cu(hfac)_2 \cdot i\text{-}PrOH$.

However, we don't use excess adduct molecules in this work, therefore, if some of the

adduct dissociate, there may not be enough ether alcohol or diol in the gas phase to cause
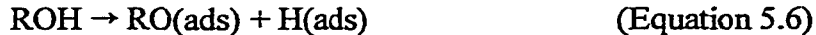
Monodentate L-L

$Cu(hfac)_2 \cdot HOCH_2CHCH_3OH$
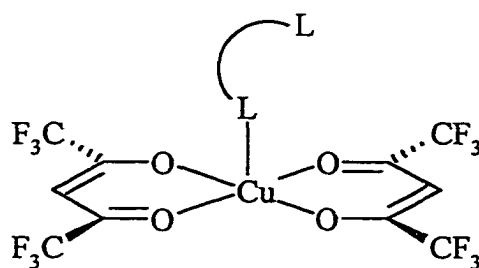
Figure 5.4

Table 5.7 CVD Results Using Adduct Precursors

Adducts	Carrier Gas	Thickness (nm)	Resistivity ($\mu\Omega \cdot$cm)
$Cu(hfac)_2 \cdot H_2O$	H_2	510	4.1
$Cu(hfac)_2 \cdot$ethylene glycol	H_2	Thin	—
$Cu(hfac)_2 \cdot$2-methoxyethanol	H_2	670 ± 400	2.7 ± 0.2
$Cu(hfac)_2 \cdot$propylene glycol	H_2	1200 ± 400	2.1 ± 0.5
$Cu(hfac)_2 \cdot$1-methoxy-2-propanol	H_2	410 ± 120	1.5 ± 0.5

deposition to occur by self-reduction under N_2 carrier gas.

In a kinetic study of $Cu(hfac)_2$ using H_2 as a reducing gas, done by Lai and Griffin, they proposed that the rate-limiting step is the recombination of adsorbed hfac and H groups to form the volatile hfacH product (Equation 5.5).[5.12] Thus, one possible rationale for the beneficial effects of water and alcohols is that they serve as H sources, either by increasing the concentration of adsorbed H atoms on the metal surface (Equation 5.6) or by directly transferring H to hfac(ads) (Equation 5.7).

$$hfac(ads) + H(ads) \rightarrow hfacH(g) \qquad \text{(Equation 5.5)}$$

$$ROH \rightarrow RO(ads) + H(ads) \qquad \text{(Equation 5.6)}$$

$$hfac(ads) + ROH \rightarrow RO(ads) + hfacH(g) \qquad \text{(Equation 5.7)}$$

To the extent that adsorbed hfac has anionic character, Equation 5.7 is essentially an acid-base reaction. If this is the principal mechanism for enhanced CVD in the presence of alcohols and water, then ROH (R= H or alkyl) can be considered a proton-transfer catalyst.

5.4 Conclusions

We have prepared four new $Cu(hfac)_2$ adducts that can be used as Cu CVD precursors under H_2 gas. Elemental analysis indicates that there is one donor ligand coordinated to the metal center. In the thermal CVD experiments of $Cu(hfac)_2$·propylene glycol and $Cu(hfac)_2$·2-methoxyethanol, we showed that these complexes formed high quality films under H_2. We propose that the alcohol molecules aid in the deposit by providing other H sources for reduction to copper metal. They show significant improvements in the deposition rates and resistivities over $Cu(hfac)_2$·H_2O without the use of excess alcohol.

Single crystal X-ray diffraction analysis of one of these complexes, $Cu(hfac)_2$·2-methoxyethanol, shows a square pyramidal geometry in which the oxygen donor adduct molecule is coordinated in an axial fashion with the apical Cu-O bond longer than the Cu-O bonds to the in-plane chelating ligands. This implies that the oxygen donor ligands for the $Cu(hfac)_2$ adducts are monondentate.

5.5 References

[5.1] Doppelt, P.; Baum, T. H. *MRS Bulletin*, **1994**, August, 41-48.

[5.2] Cho, C. -C. U. S. Patent 5,087,485 (1992).

[5.3] Maverick, A. W.; James, A. M.; Fan, H.; Isovitsch, R. A.; Stewart, M. P.; Azene, E.; Cygan, Z. C. *ACS Symp. Ser.*, in press.

[5.4] Bertrand, J. A.; Kaplan, R. I. *Inorg. Chem.*, **1966**, *5*, 489-491.

[5.5] Belford, R. C. E.; Fenton, D. E.; Truter, M. R. *J. Chem. Soc. Dalton Trans.*, **1974**, 17-24.

[5.6] Yokoi, H.; Sai, M.; Isobe, T. *Bull. Chem. Soc. Jpn.*, **1969**, *42*, 2232-2238.

[5.7] Bushnell, G. W. *Can. J. Chem.*, **1971**, *49*, 555-561.

[5.8] Wayland, B. B.; Wisniewski, M. D. *Chem. Comm.*, **1971**, 1025-1026.

[5.9] Pradilla-Sorzano, J.; Fackler, Jr., J. P. *Inorg. Chem.*, **1974**, *13*, 39-44.

[5.10] Kovac, C. A.; Jones, C. R.; Baum, T. H.; Houle, F. A. *IBM Res. Rep. No. RJ 4174(46102)*, **1984**.

[5.11] Jose, P.; Ooi, S.; Fernando, Q. *J. Inorg. Nucl. Chem.*, **1969**, *31*, 1971-1981.

[5.12] Lai, W. G.; Xie, Y.; Griffin, G. L. *J. Electrochem. Soc.*, **1991**, *138*, 3499-3504.

[5.13] Fan, H.; Fronczek, F. R.; Maverick, A. W. unpublished results.

[5.14] Jain, A.; Kodas, T. T.; Corbitt, T. S.; Hampden-Smith, M. J. *Chem. Mater.*, **1996**, *8*, 1119-1127.

[5.15] Thompson, S. C.; Hamiltion-Cole, D. J.; Gilliland, D. D.; Hitchman, M. L.; Barnes, J. C. *Adv. Mater. Opt. Electron.*, **1992**, *1*, 81-97.

Chapter 6

Conclusions and Prospects

6.1 Introduction

This dissertation reports the results of studies of copper(I) and copper(II) complexes that can be used as precursors for copper metal CVD. It discusses the use of Cu(I) amides as potential photochemical precursors as well as $Cu(hfac)_2$ adducts that could produce high quality Cu metal films.

6.2 Cu(I) Amides

6.2.1 Clusters $[CuNR_2]_4$

The work in Chapter 2 described the successful characterization of $[CuN(SiMe_3)_2]_4$. The square planar cluster is intensely phosphorescent and the emission lifetime is long and highly sensitive to the presence of dissolved O_2. Although the cluster has very low volatility, it can be used as a CVD precursor for the deposition of copper metal. Due to its phosphorescence, we were able to induce slight photochemical enhancement under UV irradiation to produce Cu metal.

Further study of the phosphorescence of $[CuN(SiMe_3)_2]_4$ and its sensitivity to O_2 is of interest. As a result of this complex containing no oxygen or fluorine, it may be useful as a precursor for co-deposition with Al. This could help strengthen Al as an interconnecting material for smaller devices contained in integrated circuits. If a better understanding of the sensitivity of the cluster to O_2 could be achieved, it could be used as an oxygen sensor.

Chapter 3 explored the use of other Cu(I) clusters as potential chemical and photochemical vapor deposition precursors. The complexes are phosphorescent and very

88

air sensitive. Emission spectra were determined for $[CuN(i\text{-}Pr)_2]_4$ and $[CuN(t\text{-}Bu)(SiMe_3)]_4$. The complexes have pale yellow luminescence when excited at wavelengths below 400 nm. If air-sensitive precursors are usable, then it may be possible to use one of the more volatile $[CuNR_2]_4$ clusters in CVD and photoinduced CVD of Cu

6.2.2 Lower nuclearity amides $[L_nCuNR_2]_x$

In Chapter 4, the isolations of lower nuclearity Cu(I) complexes were investigated. Our attempts to prepare these complexes were plagued by the lability of Cu(I) systems, and by the presence of multiple species in solution. We attempted to prepare monomeric derivatives of $[CuN(SiMe_3)_2]_4$ by using neutral donor ligands such as dmpe, dppe, and PPh_3. However, even in the presence of donor ligand, the most common product in the reactions using CuCl and $NaN(SiMe_3)_2$ as the starting reagents was $[CuN(SiMe_3)_2]_4$.

$[Cu(CH_3CN)_4](PF_6)$ was also used as a starting material because of the ready dissociation of the acetonitrile ligands. However, it was difficult to characterize the isolated products. The side product that was isolated contained the wrong ratio of Cu to donor ligand, L (Figure 4.3).

More experiments need to be done on lower nuclearity Cu(I) complexes. If a ligand could be used that could prevent autocomplexation to higher nuclearity, then these compounds should be more volatile than the $[CuNR_2]_4$ clusters and may still be light-sensitive. However, if such a ligand needs to be chemically complicated or sterically demanding, it may be difficult to prepare target species with improved volatility.

6.3 Cu(hfac)$_2$ Adducts

We prepared and studied a new class of Cu(hfac)$_2$ adducts for use as Cu CVD precursors, as discussed in Chapter 5. The ligands that were studied are ether-alcohols and diols. We anticipated that these complexes would be six-coordinate and able to produce Cu metal without the need of a reducing carrier gas or excess ligand. However, the complexes appear to be five-coordinate, like other Cu(hfac)$_2$·L adducts. Nevertheless, they are more stable than adducts with simple alcohols such as i-PrOH. The new complexes deposit Cu metal under H$_2$ gas but not under N$_2$ gas. This means that they are not self-reducing. Even though the complexes weren't self-reducing, several of them gave higher deposition rates and better film resistivities than Cu(hfac)$_2$·H$_2$O.

Due to the versatility of Cu(hfac)$_2$ as a Lewis acid, several bases could be used as potential reducing agents for the production of Cu metal. If the proper base could be found that would stabilize its Cu(hfac)$_2$ adduct long enough, it could produce Cu metal without the need of excess adduct and H$_2$ gas.

Vita

Alicia M. James was born on April 7, 1970, to Jerry and Gladys James in New Orleans, Louisiana. She attended Southern University and A&M College where she received her bachelor of science degree in chemistry in May of 1992. In August of 1992 she began her graduate career at Louisiana State University and will receive the degree of Doctor of Philosophy on May 14, 1999. She has accepted a position at AlliedSignal in Buffalo, New York.
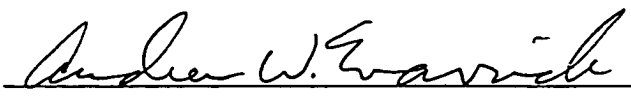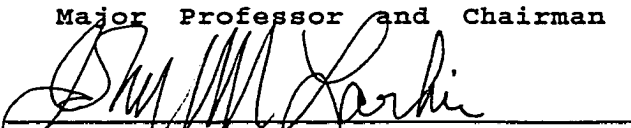
DOCTORAL EXAMINATION AND DISSERTATION REPORT

Candidate: Alicia Marie James

Major Field: Chemistry
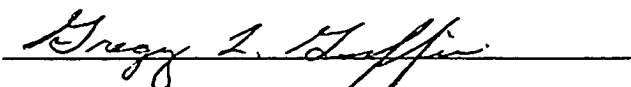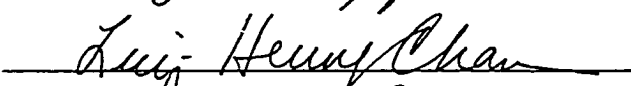
Title of Dissertation: Precursors for Chemical and Photochemical Vapor Deposition of Copper Metal

Approved:

_____
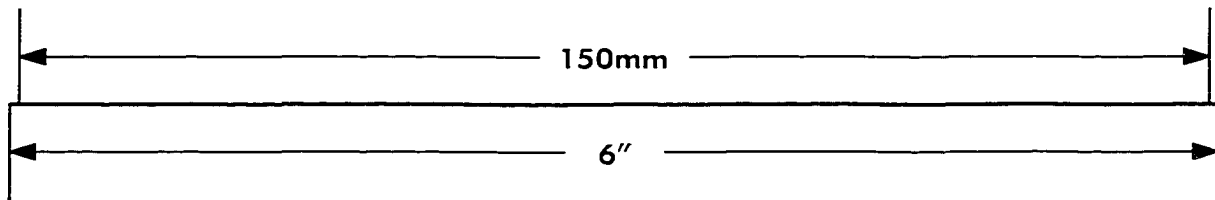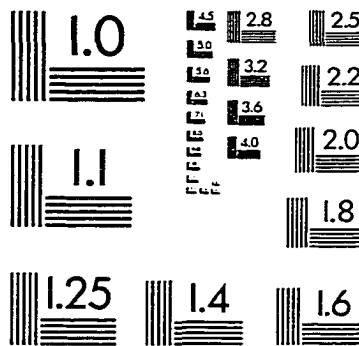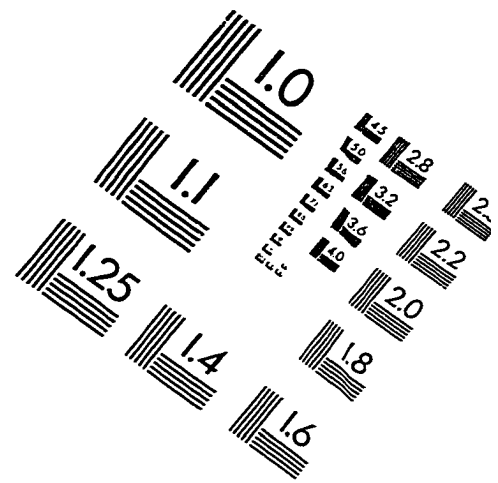Major Professor and Chairman

_____
Dean of the Graduate School

EXAMINING COMMITTEE:

_____

_____

_____

_____

_____

_____

_____

Date of Examination: _____

March 26, 1999   _____

IMAGE EVALUATION
TEST TARGET (QA-3)

150mm

6″